

Light Water Reactor Sustainability Program

Status of Cable Aging Knowledge Gaps Identified in the Expanded Materials Degradation Assessment (EMDA)



September 2023

U.S. Department of Energy

Office of Nuclear Energy

DISCLAIMER

This information was prepared as an account of work sponsored by an agency of the U.S. Government. Neither the U.S. Government nor any agency thereof, nor any of their employees, makes any warranty, expressed or implied, or assumes any legal liability or responsibility for the accuracy, completeness, or usefulness, of any information, apparatus, product, or process disclosed, or represents that its use would not infringe privately owned rights. References herein to any specific commercial product, process, or service by trade name, trademark, manufacturer, or otherwise, does not necessarily constitute or imply its endorsement, recommendation, or favoring by the U.S. Government or any agency thereof. The views and opinions of authors expressed herein do not necessarily state or reflect those of the U.S. Government or any agency thereof.

Status of Cable Aging Knowledge Gaps Identified in the Expanded Materials Degradation Assessment (EMDA)

Leonard S. Fifield, Yelin Ni, Mychal P. Spencer

September 2023

**Prepared for the
U.S. Department of Energy
Office of Nuclear Energy**

EXECUTIVE SUMMARY

This report summarizes research relevant to cable aging knowledge gaps identified in NUREG/CR-7153, “Expanded Materials Degradation Assessment (EMDA) Volume 5: Aging of Cables and Cable Systems” (EMDA Vol. 5), performed since the EMDA Vol. 5 was published in 2014. It begins with a discussion of the status of cables in long-term operation of U.S. nuclear power plants (NPPs) and the most common cables found in NPP containment. Next, the major polymer cable insulations, and the mechanisms of concern for degradation of those polymers in service are reviewed. A description of the environmental qualification (EQ) process historically used for safety-related cables is provided as is a review of the potential concerns with that process highlighted in the EMDA Vol. 5. Research addressing each of these is then reviewed. Finally, three potential strategies to support continued safe operation of aging cables are proposed: advanced condition-based verification, targeted material aging studies, and predictive simulation.

The most important properties of cable insulation are dielectric strength and mechanical durability. Mechanisms of deterioration of dielectric and mechanical properties are presented herein, which vary between crosslinked polyethylene (XLPE) and ethylene propylene rubber (EPR)-type insulations based on differences in their molecular structure and product formulation. Reviewing the degradation mechanisms of thermal and radiation aging provides a unified and systematic knowledge base to explain anomalous phenomena identified as knowledge gaps.

Degradation due to moisture and affected dielectric properties is a distinct area of interest from thermal-radiation aging. Electric Power Research Institute (EPRI) guidelines on Tan Delta testing and acceptance criteria were statistically examined and confirmed as a primary tool for condition monitoring of medium voltage (MV) cables in wet or submerged environments.

Environmental service condition data collected by EPRI concluded that the actual temperatures and integrated total dose are lower than design values [40 ~ 50 °C, 50 Mrad (500 kGy)].

Knowledge gaps identified in the EMDA Vol. 5 represent concerns that the assumptions made in 40-year environmental qualification of cables may be weak, that the pre-aging of cables prior to loss of coolant accident (LOCA) testing may have represented less than 40-year equivalence, and that consequently the EQ process may not be conservative and thereby overpredict cable useful lifetime. While cable failures are historically few in the first 40-60 years of plant operation, the concern is that lack of conservatism in the 40-year qualification is a more serious issue in licensing up to 80 years. Subsequent research by the U.S. Department of Energy (DOE) and others in the years following publication of the EMDA Vol. 5, as reviewed herein, found that the Arrhenius and equal dose/equal damage assumptions of thermal and radiation aging behavior on which the historical qualification process was based hold for some relevant cable materials, accelerated aging conditions, and performance metrics and do not hold for others. While the pre-aging process appears to be not conservative in some cases, it appeared to be conservative in others.

Three approaches to increase confidence in the continued reliable performance of existing nuclear electrical cables are: 1) advance comprehensive cable condition monitoring programs using existing and newly developed tools to inform decisions to repair, replace, or retain aged cables, 2) pursue additional aging studies and the characterization of harvested materials for greater understanding of nuclear cable insulation degradation in the nuclear plant environment, and 3) utilize modeling and simulation to predict cable performance from material measures. Use of a testing-based approach is anticipated to be the most promising strategy for future cable aging management in light water reactors—supported by targeted material aging studies, modeling and simulation of material composition/exposure/performance relationships, and evaluation of harvested cables.

ACKNOWLEDGEMENTS

This work was sponsored by the U.S. Department of Energy, Office of Nuclear Energy, for the Light Water Reactor Sustainability (LWRS) Program Materials Research Pathway. The authors extend their appreciation to Pathway Lead Dr. Xiang (Frank) Chen for LWRS programmatic support and Andrew Mantey of the Electric Power Research Institute for his review. This work was performed at the Pacific Northwest National Laboratory (PNNL). PNNL is operated by Battelle for the U.S. Department of Energy under contract DE-AC05-76RL01830.

CONTENTS

1.	Background.....	12
2.	NPP Electrical Cables and Their Polymers	14
2.1	Electrical Cables	14
2.2	Database of Insulation Material Types	15
2.2.1	SAND96-0344	15
2.2.2	EPRI-TR-103841	15
2.2.3	NEI 06-05.....	16
2.3	Typical XLPE and EPR/EPDM Insulation Formulations.....	17
2.4	Crosslinking in Polymers	18
2.4.1	Radiation Crosslinking.....	18
2.4.2	Peroxide Crosslinking.....	19
2.4.3	Silane Crosslinking	19
2.4.4	Azo Crosslinking.....	19
3.	Polymer Degradation Mechanisms.....	20
3.1	Basic Autoxidation Scheme	20
3.2	Effect of Degradation on Mechanical Properties	21
3.3	Effect of Degradation on Insulation Function.....	23
4.	Cable Aging in Qualification.....	24
4.1	Qualification Standards.....	24
4.2	Accelerated Aging Model Assumptions	26
5.	Cable Aging Knowledge Gaps	26
5.1	Deviations from Arrhenius Temperature Dependence.....	27
5.1.1	Diffusion Limited Oxidation (DLO).....	27
5.1.2	Non-Arrhenius Behaviors at Low Temperatures	28
5.1.3	Uncertainties and Variabilities.....	30
5.2	Equal Dose, Equal Damage Assumption	30
5.2.1	Dose Rate Effects.....	31
5.3	Synergism of Thermal and Radiation Aging	32
5.3.1	Synergism of Thermal and Radiation Aging	32
5.3.2	Inverse Temperature Effects (ITE)	35
5.4	Moisture Effects.....	37
5.5	Actual NPP Environments	38
6.	Path Forward on EMDA Vol. 5 Knowledge Gaps	38
6.1	Advanced Aging Studies.....	38
6.1.1	Improved Accelerated Aging	39
6.1.2	Better Understanding of Cable Environments	40
6.1.3	Harvested Cables.....	40
6.2	Modeling for Cable Performance Prediction	40
6.3	Condition Based Decision Making	42
7.	Summary.....	44
8.	References	46

FIGURES

Figure 1. Number of units by expiration year of current renewed license requiring SLR before year 2029 – 2042 [2].	12
Figure 2. Cables commonly found in NPPs and the voltage ratings for power cables. *see discussion of MV in text.	14
Figure 3. Material types and percentage of units with in-containment cable insulation polymers. Acronyms have the same definitions as in Table 2 [12].	16
Figure 4. Underground MV cable insulation types by voltage and number of units reporting the material [13].	17
Figure 5. Failure of MVU cables versus years of installation categorized by insulation type [13].	17
Figure 6. Chemical structures of EPR and EPDM with different diene monomer side chains [17].	18
Figure 7. Process for crosslinking of XLPE due to irradiation.	19
Figure 8. Diagram of XLPE formed with vinyltrimethoxysilane (VTMS) [24].	19
Figure 9. Basic autoxidation scheme (BAS) for polymers.	20
Figure 10. Disproportion of two PE radical chains [17].	21
Figure 11. Scission of polyolefin backbone during photooxidation [29].	21
Figure 12. (a)(b) Material properties of an XLPE film changing with aging time at 120 °C. Tensile stress-strain curves of (c) XLPE and (d) EPR films aged at 120 °C for up to 41 hours [32].	22
Figure 13. Cracking of polymer jacket and insulation in bend regions as circled in yellow. Photo courtesy: EPRI – cable harvesting guide, https://cableharvest.epri.com/index.html (registration required).	23
Figure 14. Chemical potential as a function of conductivity [37].	24
Figure 15. Type testing to qualify for normal operation described in IEEE Std 383-1974.	25
Figure 16. Type testing for operation during DBE described in IEEE Std 383-1974.	26
Figure 17. (Left) Color change in the cross-sections of tubular insulation specimens after thermal aging. (Top-right) Through-thickness total color difference (ΔE_{ab}^*) of EPR samples aged at 165 °C with respect to the color of unaged sample and (bottom-right) oxygen concentration measured by energy dispersive X-ray spectroscopy through thickness [57].	28
Figure 18. Deviations from Arrhenius temperature dependence above 150 °C and below 100 °C [58].	29
Figure 19. Deviations from Arrhenius temperature dependences evident by (a) EAB of a chloroprene rubber jacket [61] and (b) oxygen (O ₂) consumption of another chloroprene rubber with fewer fillers [53].	29
Figure 20. Illustration of dose rate effects present in an EAB dataset [66].	31
Figure 21. Illustration of the onset dose rate (dashed lines) for dose rate effect at different temperatures.	31
Figure 22. Normalized EAB with total dose for (a) XLPE and (b) EPDM aged at three conditions: T/R: 150 °C and 300 Gy/h (30 Mrad/h) simultaneously, T+R: thermal-only aging at 150 °C, followed by radiation aging at 300 Gy/h (30 Mrad/h) and room temperature (26	

°C), and R+T: the reverse of T+R. Mass change relative to the unaged samples for (c) XLPE and (d) EPDM after the same aging conditions [76].	33
Figure 23. Normalized EAB with respect to aging time in sequential and simultaneous aging conditions: “T” means thermal aging at 120 °C and “R” refers to radiation aging at 650 Gy/h (65 Mrad/h). The number beside “R” refers to the temperature in °C during radiation aging. The highlighted datapoints showed an increase in EAB [74].	34
Figure 24. Carbonyl index, total color difference and indentation modulus of XLPE and EPDM subjected to simultaneous (T/R), sequential (T+R) and reversed simultaneous (R+T) aging. The temperatures and dose rates are the same as in Figure 22 [76].	34
Figure 25. Recovery of EAB upon annealing at 140 °C for 24 h, after room temperature (22 °C) radiation aging at 200 Gy/h (20 Mrad/h) [79,80].	35
Figure 26. Normalized EAB of (a) XLPE and (b) EPDM aged at 100 Gy/h (10 Mrad/h) and 26 °C, 50 °C, 90 °C [81].	36
Figure 28. Superposition of normalized EAB isotherms when plotted against oxygen consumption of (a) neoprene and (b) XLPO samples. EAB data were obtained in SCRAPS with sample ID (a) “Neo-02” and (b) “XLPO-02A” [90]. Oxygen consumption data were found in published papers and reports [61,92].	39
Figure 29. (a) Dose to reach 100% EAB of an EPR material with aging temperature in °C marked beside the data points. (b) Horizontally shifting the data to 50 °C. Filled symbols represent shifted results. [94].	41
Figure 30. Dose to equivalent damage as a function of dose rate predicted by different models. [95]	42
Figure 30. Illustration of dichotomy model [96].	42

TABLES

Table 1. Polymer-based electrical components listed in VI.A. and VI.B. of NUREG-2191 [3].	13
Table 2. Polymer types used as cable insulation found in EPRI NUS Cable Database [11].	15
Table 3. IEEE Std 323 and IEEE Std 383 releases and endorsements by the NRC.	25
Table 4. Cable aging knowledge gaps originating from unsatisfied phenomenological model assumptions.	27

ACRONYMS

AMP	aging management program
ASTM	American Society for Testing and Materials
BAS	basic autoxidation scheme
CBQ	condition-based qualification
CFR	Code of Federal Regulations
CPE	chlorinated polyethylene
CSPE	chlorosulfonated polyethylene
DBE	design basis event
DC	direct current
DCP	dicumyl peroxide
DED	dose to equivalent damage
DLO	diffusion limited oxidation
DOE	Department of Energy
EAB	elongation at break
EDS	energy dispersive X-ray spectroscopy
EMDA	Expanded Materials Degradation Assessment
EPDM	ethylene propylene diene monomer
EPR	ethylene propylene rubber
EPRI	Electric Power Research Institute
EQ	environmental qualification
FOA	Funding Opportunity Announcement
FTIR	Fourier-transform infrared
GALL	Generic Aging Lessons Learned
HV	high voltage
I&C	instrumentation and control
IEEE	Institute of Electrical and Electronics Engineers
IEEE Std	IEEE Standard
ITE	inverse temperature effects
LDPE	low density polyethylene
LV	low voltage
LWRS	Light Water Reactor Sustainability
MAC	matched accelerated condition
MV	medium voltage

MVU	medium voltage underground
NEI	Nuclear Energy Institute
NPP	nuclear power plant
NRC	Nuclear Regulatory Commission
NEUP	Nuclear Energy University Program
PE	polyethylene
PNNL	Pacific Northwest National Laboratory
PP	polypropylene
PVC	polyvinyl chloride
PILC	paper insulated lead jacketed cable
RG	regulatory guide
SCRAPS	Sandia's Cable Repository of Aged Polymer Samples
SLR	subsequent license renewal
SR	silicon rubber
TR-XLPE	tree-retardant crosslinked polyethylene
TLAA	time-limited aging analyses
XLPE	crosslinked polyethylene
XLPO	crosslinked polyolefin

1. Background

Commercial nuclear power plants (NPPs) were initially licensed to operate for up to 40 years. Most reactors in the United States have had their licenses renewed to operate for up to 60 years and first approvals of subsequent license renewals to operate up to 80 years have begun [1]. Each renewed license seeks to maintain safe NPP operation in accordance with the initial license. Figure 1 shows the number of units that have been issued a license renewal (for 40 – 60 year operation) and will require a subsequent license renewal (SLR, for 60 – 80 year operation) categorized by the expiration of their current licenses.

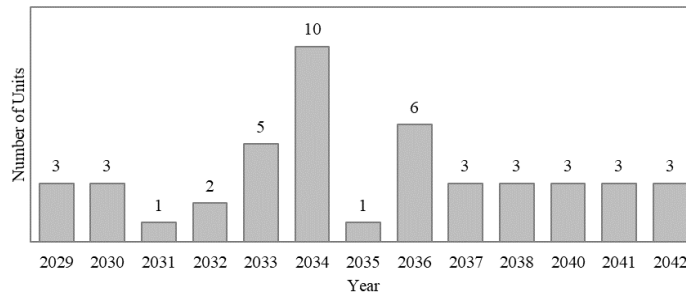


Figure 1. Number of units by expiration year of current renewed license requiring SLR before year 2029 – 2042 [2].

Requirements for both initial and subsequent license renewal are established by the Code of Federal Regulations (10 CFR) Part 54, where § 54.29 specifies “managing the effects of aging” and “time-limited aging analyses” (TLAA) as the standards for issuance of a renewed license. In § 54.21 “contents of application – technical information”, aging management programs (AMPs) and TLAA are required to be part of a written document submitted to the U.S. Nuclear Regulatory Commission (NRC) for SLR application. NUREG-2191, “Generic Aging Lessons Learned for Subsequent License Renewal (GALL-SLR),” provides guidance on the content of the SLR application [3]. Chapters II through VIII of the GALL-SLR report contain AMP guidance for seven major categories of the structures and components in NPPs. Chapter VI, “Electrical Components”, lists itemized components made of different materials and subjected to various environments, the aging effects on these items, and corresponding AMPs referring to a sub-section in Chapters X and XI. Items relevant to polymer-based electrical insulations from GALL-SLR are recapitulated in Table 1.

The AMP X.E1 in NUREG-2191 demonstrates acceptability of TLAA to extend the qualified life of equipment subjected to 10 CFR 50.49 environmental qualification (EQ) requirements, covering safety-related electric equipment per 10 CFR 50.49(b)(1), including Class 1E cables as defined in IEEE Std 323. The reanalysis of initial EQ data may be used to establish qualification for life extension if excess conservatism were incorporated in the initial evaluation; otherwise, replacement or requalification of the cables is required. Sources of conservatism include the anticipated design environments (temperature and total integrated dose) being more severe compared to actual environmental data gathered in operating plants, as well as conservatism in activation energy values for pre-aging used in the initial qualification analysis.

Compared to NUREG-1801, Rev. 2, “Generic Aging Lessons Learned (GALL)” published in December 2010 [4], the AMP X.E1 in NUREG-2191 added the consideration of unquantified uncertainties in the accelerated aging of electrical cables, such as diffusion limited oxidation, activation energy, synergistic effects, inverse temperature, and dose rate effects. These additional considerations were identified as potential concerns in qualification methodology/gaps in knowledge for long-term NPP operation in the Expanded Materials Degradation Assessment (EMDA): Aging of Cables and Cable Systems (NUREG/CR-7153, Volume 5) (EMDA Vol. 5) [5]. These knowledge gaps are situations where the Arrhenius or the dose integration methodologies do not hold, and where additional research was suggested.

Table 1. Polymer-based electrical components listed in VI.A. and VI.B. of NUREG-2191 [3].

Table VI.B Equipment Subject to 10 CFR 50.49 Environmental Qualification Requirements					
Structure and/or Component	Material	Environment	Aging Effect/Mechanism	Aging Management Program (AMP)/TLAA	
Electrical equipment subject to 10CFR 50.49 EQ requirements	Various polymeric and metallic materials	Areas of the plant that could be subjected to harsh environmental effect of a loss of coolant accident (LOCA), high energy line break, or post LOCA environment. Adverse localized environment (e.g., temperature, radiation, or moisture)	Various aging effects due to various mechanisms in accordance with 10 CFR 50.49	EQ is a time-limited aging analysis (TLAA) to be evaluated for the subsequent period of extended operation. See the standard review plan, Section 4.4, "Environment Qualification (EQ) of Electric Equipment," for acceptable methods for meeting the requirements of 10 CFR 54.21(c)(1) and (ii) See AMP X.E1. "Environmental Qualification (EQ) of electric Equipment," of this report for meeting the requirements of 10 CFR 54.21(c)(1)(iii)	
Table VI.A Equipment Not Subject to 10 CFR 50.49 Environmental Qualification Requirements					
Structure and/or Component	Material	Environment	Aging Effect/Mechanism	Aging Management Program (AMP)/ TLAA	
Electrical insulation for electrical cables and connections (including terminal blocks, etc.)	Various organic polymers (e.g., EPR, SR, EPDM, XLPE)	Adverse localized environment caused by heat, radiation, or moisture	Reduced electrical insulation resistance due to thermal or thermoxidative degradation of organics, radiolysis, and photolysis (UV sensitive materials only) of organics; radiation-induced oxidation; moisture intrusion	AMP XI.E1, "Electrical Insulation for Electrical Cables and Connections Not Subject to 10 CFR 50.49 Environmental Qualification Requirements"	
Electrical insulation for electrical cables and connections used in instrumentation circuits that are sensitive to reduction in conductor electrical insulation resistance				AMP XI.E2, "Electrical Insulation for Electrical Cables and Connections Not Subject to 10 CFR 50.49 Environmental Qualification Requirements Used in Instrumentation Circuits"	
Electrical conductor insulation for inaccessible medium-voltage cables-typical operating range of 2kV to 35 kV (e.g., installed in duct bank, buried conduit or direct buried)	Various organic polymers such as EPR, SR, EPDM, XLPE, butyl rubber, and combined thermoplastic jacket/ insulation shield	Adverse localized environment caused by significant moisture	Reduced electrical insulation resistance or degraded dielectric strength due to significant moisture	AMP XI.E3A, "Electrical Insulation for Inaccessible Medium-Voltage Power Cables Not Subject to 10 CFR 50.49 Environmental Qualification Requirements"	
Electrical conductor insulation for inaccessible instrumentation and control cables (e.g., installed in duct bank, buried conduit or direct buried)				AMP XI.E3B, "Electrical Insulation for Inaccessible Instrument and Control Cables Not Subject to 10 CFR 50.49 Environmental Qualification Requirements"	
Electrical conductor insulation for inaccessible low-voltage cables-typical operating range of < 1kV but no greater than 2 kV (e.g., installed in duct bank, buried conduit or direct buried)				AMP XI.E3C, "Electrical Insulation for Inaccessible Low-Voltage Power Cables Not Subject to 10 CFR 50.49 Environmental Qualification Requirements"	
Metal enclosed bus: electrical insulation; electrical insulators	Porcelain; xenoy; thermoplastic organic polymers	Air – indoor controlled or uncontrolled, air – outdoor	Reduced electrical insulation resistance due to thermal or thermoxidative degradation of organics or thermoplastics, radiation-induced oxidation, moisture or debris intrusion, ohmic heating	AMP XI.E4, "Metal Enclosed Bus"	
Metal enclosed bus: enclosure assemblies	Elastomer			Surface cracking, crazing, scuffing, dimensional change (e.g., "ballooning" and "necking"), shrinkage, discoloration, hardening, loss of strength due to elastomer degradation	AMP XI.E4, "Metal Enclosed Bus," or AMP XI.M38, "Inspection of Internal Surfaces in Miscellaneous Piping and Ducting Components"
Cable Bus	Electrical insulation; insulators			Reduced electrical insulation resistance due to thermal/ thermoxidative degradation of organics and photolysis (UV sensitive materials only) of organics, moisture/ debris intrusion and ohmic heating	A plant-specific aging management program is to be evaluated

Further investigation of cable aging knowledge gaps to support regulatory decisions related to SLR supports the mission of the Light Water Reactor Sustainability (LWRS) program of the U.S. Department of Energy (DOE) Office of Nuclear Energy [6]. As such, research on cable aging knowledge gaps has been conducted under the LWRS Materials Research Pathway (MRP). This report, as a task under the MRP, provides a summary of the research outcomes on the cable aging knowledge gaps identified in EMDA Vol. 5, with a focus on recent findings (since 2010), especially in programs sponsored by DOE. Other published reports and journal papers relevant to knowledge gaps are also included. The objective of this report is to provide an update on research observations during lab testing and to consider recommendations for future work. This report is not intended to modify existing EQ, TLAA, or AMP guidance, nor to establish any qualification or lifetime extension methods.

2. NPP Electrical Cables and Their Polymers

NPP electrical cable designs typically include a conductor to carry power, instrumentation, or control signals, and an insulating cover layer to isolate the conductor. They may include more than one insulated conductor within an assembly. Other components that may be associated with the overall cable design include a semiconductor screen, a shield over each conductor and/or over all conductors, binder tape, and a jacket. While the insulation provides electrical isolation, in jacketed cable configurations the jacket serves to provide mechanical protection during installation and may provide fire or moisture resistance depending on the cable construction.

2.1 Electrical Cables

In this report, materials of interest are polymer-based insulation for low-voltage (LV) power cables, medium-voltage (MV) power cables, and instrumentation and control (I&C) cables that typically operate at LV. Figure 2 shows common categories of cables used in NPPs and voltage ratings for power cables. Note that industrial definitions for voltage ranges categorized as MV vary. For example, NUREG-2191 Chapter VI-A specifies typical operating voltage of MV power cables to be 2 kV to 35 kV [3]. However, on IEEE online dictionary referring to IEEE Std 690-2018, a standard for cable systems for Class 1E circuits, MV power cables are defined as “designed to supply power to devices of plant systems rated 2 kV to 15 kV” [7,8]. In addition, ICEA S-94-649 specifies “medium voltage shielded power cables” as “rated 5 kV to 46 kV” [9]. Lastly, EPRI TR 3002005322 specifies MV as 5 kV to 46 kV, and low voltage power cable as lower than 2 kV [10].

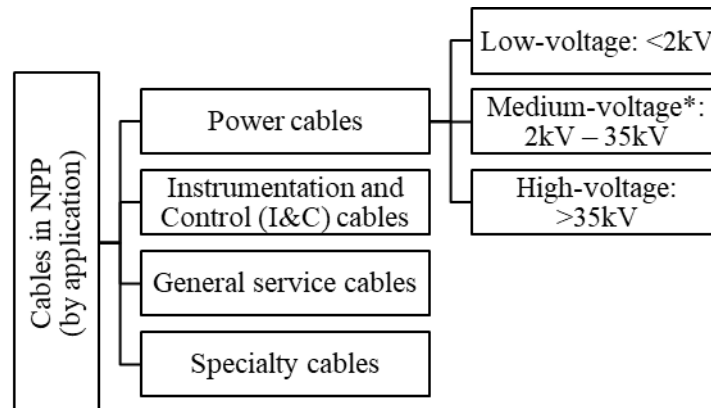


Figure 2. Cables commonly found in NPPs and the voltage ratings for power cables. *see discussion of MV in text.

2.2 Database of Insulation Material Types

Crosslinked polyethylene (XLPE) and ethylene propylene, including ethylene propylene rubber (EPR) and ethylene propylene diene monomer (EPDM) rubber, are the most common polymeric cable insulation materials in NPPs based on the following three references, discussed in detail below.

- [SAND96-0344](#), “Aging Management Guideline for Commercial Nuclear Power Plants Electrical Cable and Terminations”, published in 1996 [11].
- [EPRI-TR-103841](#), “Low-Voltage Environmentally-Qualified Cable License Renewal Industry Report; Revision 1”, published in 1994 [12].
- [NEI 06-05](#), “Medium Voltage Underground Cable White Paper”, published in 2006 [13].

2.2.1 SAND96-0344

In SAND96-0344 [11], a sorting was performed on an “EPRI NUS Cable Database” to look at the most common types of insulating polymers and the results are given in Table 2. The EPRI database is a listing of EQ cables installed in EPRI-member NPPs. The sorted results were obtained in April 1993, covering 67 plants and 101 units. Approximately 89% of U.S. units operating at that time are represented in the database and 1215 out of 1660 database entries listed the insulation materials. According to Table 2, XLPE and EPR were the most numerous insulation material types.

Table 2. Polymer types used as cable insulation found in EPRI NUS Cable Database [11].

Insulation Material	No. of Database Entries	% of Total
XLPE, crosslinked polyethylene	439	35.9
EPR, ethylene propylene rubber	434	35.5
SR, silicone rubber	63	5.2
Kerite	61	5.0
PE, polyethylene	52	4.3
ETFE, ethylene tetrafluoroethylene	39	3.2
FR, flame retardant	36	2.9
CSPE, chlorosulfonated polyethylene	28	2.3
BR, butyl rubber	20	1.6
PVC, polyvinyl chloride	12	1.0
Mineral	12	1.0
Polyimide	8	<1.0
Polypropylene	3	<1.0
XLN, crosslinked neoprene	3	<1.0
Industrite	2	<1.0
Neoprene	2	<1.0
Styrene	1	<1.0
Total	1215	100

2.2.2 EPRI-TR-103841

A different analysis approach than that used in SAND96-0344 is presented in EPRI-TR-103841 [12]. The polymer types used as cable insulation materials were sorted in a bar chart, as shown in Figure 3, where each bar represents the percentage of units possessing the particular type of in-containment cable insulation polymer. The results presented in Figure 3 were based upon data in an in-containment cable

database initially developed from an EPRI EQ data bank and supplemented with information obtained over the years by cable experts at Sandia National Laboratories [12]. The database was described to contain information on in-containment cables at 106 nuclear power plants [12] whose construction permits dated between 1957 and 1978. The conclusion drawn from the figure is that XLPE and EPR/EPDM are the two most popular insulation material types, found in approximately 90% and > 70% of units, respectively.

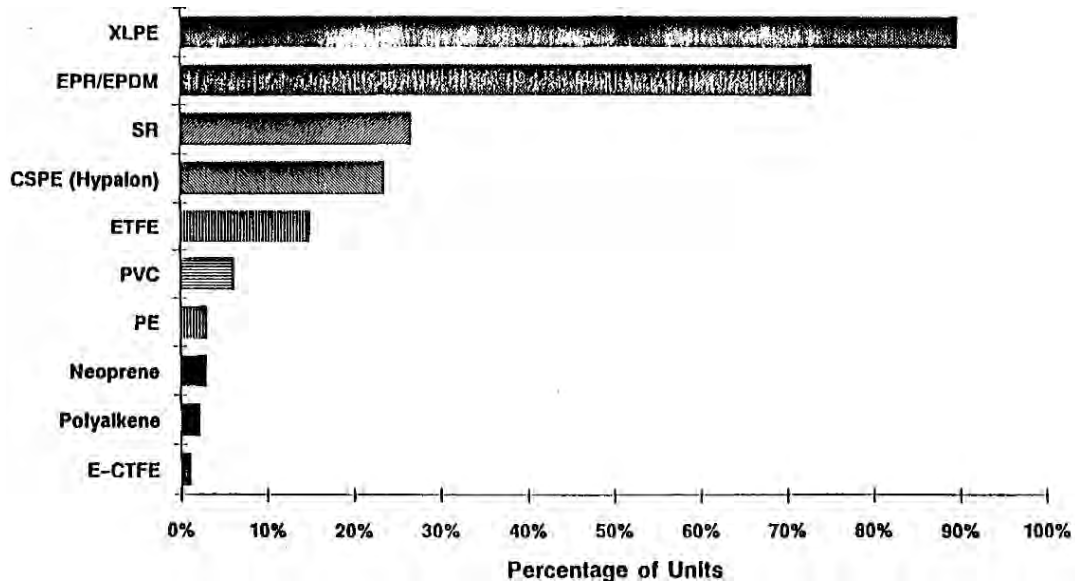


Figure 3. Material types and percentage of units with in-containment cable insulation polymers. Acronyms have the same definitions as in Table 2 [12].

2.2.3 NEI 06-05

In NEI 06-05 [13], a survey was conducted of MV underground (MVU) cables in 2005 to identify MVU cable types (voltage ratings) in use, insulation materials, and failure occurrence and causes. The survey received responses from 81 units, which represented 51 plants. The survey results presented in the report are replotted in Figure 4. The predominant polymer type used as MVU cable insulation was EPR, including black, brown, and red variations. The red EPR in the NEI survey is often called “pink EPR” [14] in other reports including in the EMDA Vol. 5. The number of units reporting each insulation material is also given in Figure 4. In addition, the survey reported the age of MVU cables at failure, as plotted in Figure 5 for each insulation polymer type. From Figure 5, early failures were observed to occur with MV cables in a wet condition. Furthermore, it was concluded that failures of EPR in general were related to flaws such as manufacturing defects and installation damage combined with wet conditions, rather than wetting alone.

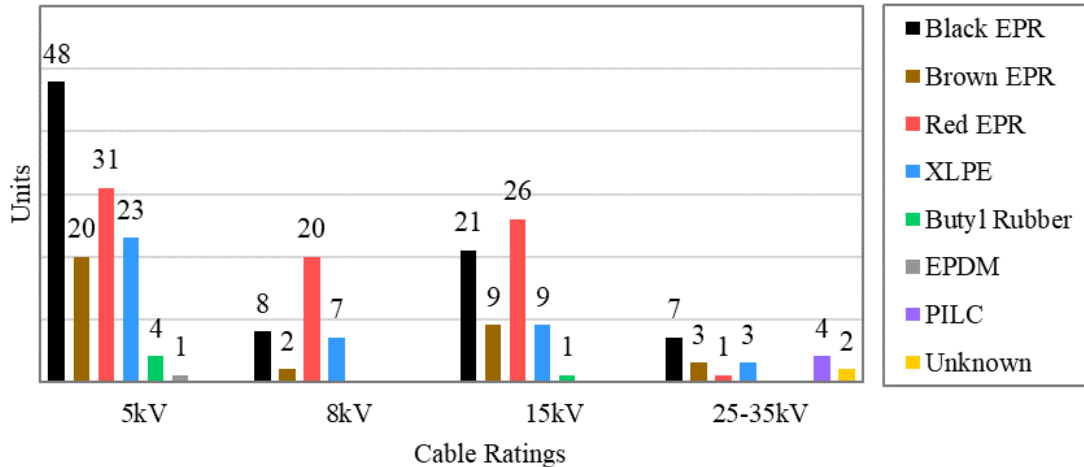


Figure 4. Underground MV cable insulation types by voltage and number of units reporting the material [13].

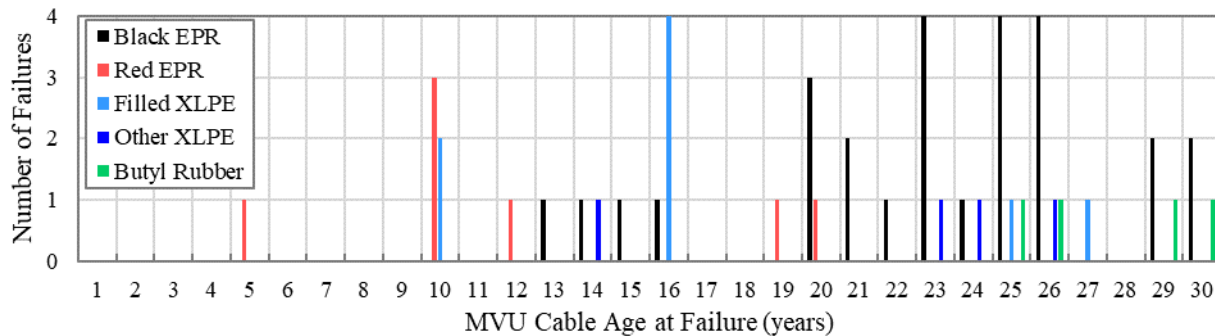


Figure 5. Failure of MVU cables versus years of installation categorized by insulation type [13].

2.3 Typical XLPE and EPR/EPDM Insulation Formulations

In NPP electrical cables, XLPE may be used in a relatively pure form [15], although some formulations such as Vulkene[®] are mineral filled [16]. The formulation of EPR/EPDM is complex compared to XLPE as EPR/EPDM may consist of over 50% additives by weight [15]. Also, EPR can be purely amorphous or semi-crystalline with > 55% ethylene content [17]. While EPDM has diene groups that allow sulfur vulcanization, sulfur curing is not commonly used for MV cable insulation [16] since peroxide cured EPDM has superior dielectric properties after long-term immersion in hot water [15,18]. Fillers are the most abundant additive type and the key component to performance of EPR/EPDM [10,18]. Without fillers, the polymer matrix alone is soft, leading to melt fracture during extrusion and lack of processibility, in addition to low mechanical modulus and strength of the end product [18]. The chemical structures of EPR and EPDM are shown in Figure 6.

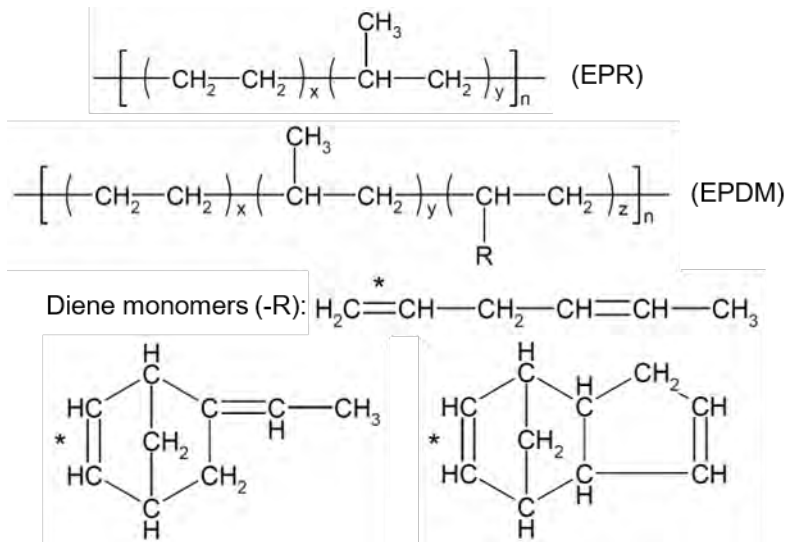


Figure 6. Chemical structures of EPR and EPDM with different diene monomer side chains [17].

2.4 Crosslinking in Polymers

The properties of polymeric insulation, especially XLPE-type insulation, are strongly influenced by its crosslinking, including the approach to crosslinking and the crosslink density. With variations in crosslink density, the degree of crystallinity, mechanical strength and elongation, dielectric strength, water-tree retardance, and more will vary. In general, the increase of crosslinking density with higher radiation dose [typically above 100 kGy (10 Mrad)] leads to a decrease in tensile elongation at break (EAB) and an increase in tensile strength [19,20]. It has been reported that tensile strength increases initially and then decreases with dose [100 – 200 kGy (10 – 20 Mrad)] [21], while EAB only decreases. With an increase in crosslink density, decrease in breakdown voltage and breakdown strength have also been reported [22].

Crosslinking involves a pair of free radicals on two polymer chains forming a new C-C bond. In terms of XLPE, the free radicals can be generated from (1) radiation, (2) peroxides, (3) silane compounds, and (4) azo compounds [23], which are discussed further below. EPR is normally cured by electron beam (E-beam) radiation (2.4.1) or thermally using peroxides (2.4.2) [17].

2.4.1 Radiation Crosslinking

The radiation crosslinking mechanism of XLPE is shown in Figure 7. The first step is initiation, where the C-H bond breaks after absorbing high-energy photons during irradiation and a polymer radical is formed as a result. The second step occurs when a C-C bond is formed due to the interaction of two polymer radicals. Radiation crosslinking does not require high temperature and can occur in the solid phase. Furthermore, the crystalline phase of the polymer remains largely intact following crosslinking, which supplies a relatively high chemical resistance and improved mechanical properties. Radiation crosslinked XLPE has been commonly used for LV cable insulation [15]. The source of radiation can be gamma ray, X-ray, electron beam, or ultraviolet [23]. The relevant source of radiation exposure for cables in NPPs is primarily gamma ray and this exposure may cause further crosslinking of in-use XLPE, potentially leading to embrittlement and failure.

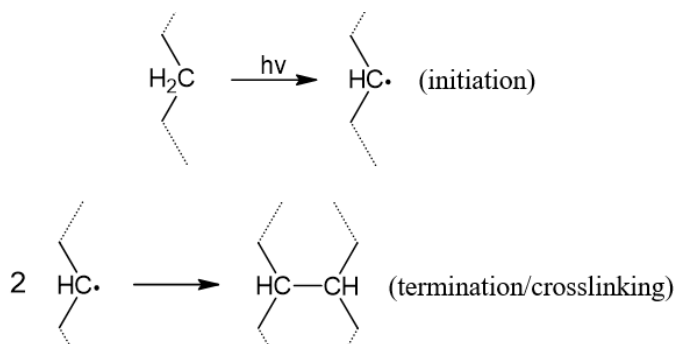


Figure 7. Process for crosslinking of XLPE due to irradiation.

2.4.2 Peroxide Crosslinking

Peroxide crosslinking follows the same free radical reaction as shown in Figure 7, except that the free radicals are generated by thermal decomposition of peroxides. The peroxide radicals ($\text{RO}\cdot$) abstract the hydrogen in PE and produced polymer radicals. Since peroxide crosslinking occurs in the melt state, the network structure of peroxide crosslinked XLPE is more homogeneous than radiation crosslinked XLPE [23].

2.4.3 Silane Crosslinking

Silane crosslinking involves three steps: (i) initiation of PE radicals by radiation or peroxides as discussed above, (ii) grafting of silanes such as vinyltriethoxysilane (VTES) or vinyltrimethoxysilane (VTMS) onto PE chains, and (iii) formation of Si-O-Si crosslinking bonds by silane hydrolysis and silanol condensation [23,24]. Figure 8 illustrates these steps for VTMS. Note that formation of crosslinkable silanol groups from alkoxy groups requires water, which is typically introduced via a hot water bath or steam treatment [24]. Any remaining water in the XLPE with silane crosslinking can lead to a reduction in dielectric strength and early degradation, which is unfavorable for cable insulation.

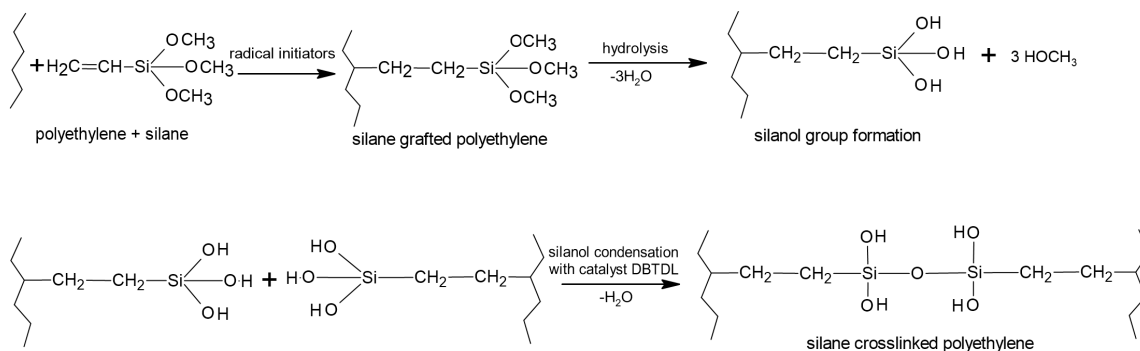


Figure 8. Diagram of XLPE formed with vinyltrimethoxysilane (VTMS) [24].

2.4.4 Azo Crosslinking

Azo crosslinking uses azo compounds as an initiator which are more thermally stable than peroxides [23]. In addition, azo crosslinking allows higher extrusion temperature and is suitable for high molecular weight PE [23]. For cable insulation materials, which are typically based on low-density PE (LDPE), use of azo crosslinking is not common.

3. Polymer Degradation Mechanisms

On a microscopic level, the aging or degradation of polymer insulation is a chemical process that is not significantly different from free radical reactions that form molecular crosslinks. The basic autoxidation scheme (BAS) is the simplest model to describe oxidative degradation [25]. However, physical processes such as diffusion of oxygen are not considered in the BAS. Oxidative degradation may lead to macroscopic deterioration in insulation performance such as mechanical embrittlement (e.g., cracking). Micro-voids formed by mechanical cracking or crazing can lead to a decrease in insulation resistivity, water-treeing, and even dielectric breakdown. With the free radical crosslinking process discussed in Section 2.4, this section focuses on the free radical depolymerization mechanism involving initiation, propagation, and termination on the aging of cable insulation polymers. Subsequently, effects of oxidative degradation on polymers are discussed in terms of mechanical and dielectric properties.

3.1 Basic Autoxidation Scheme

The basic autoxidation scheme (BAS) of Bolland and Gee was first proposed for lipids and rubbers [26–28]. It has been widely accepted to describe the oxidative degradation of polymers in a chain process of initiation, propagation, transfer or branching, and termination, as listed in Figure 9.

Free radicals (\bullet) can be generated from multiple environmental stressors in NPPs, mostly radiation and heat. Initiation through radiation is the same process as described above and any chemical bond can be activated through radiation. Initiation through heat, on the other hand, typically occurs upon decomposition of a thermodynamically less stable bond and is slower and more selective than photo-initiation. In terms of radical propagation, a peroxy radical ($RO_2 \bullet$), which is more stable than an alkyl radical ($R \bullet$), is first formed in the presence of oxygen. Next, the radical can propagate to another polymer chain via H-atom transfer. If an allylic H is abstracted from a second polymer chain, the radicals formed ($R' \bullet$ in step 3 of BAS in Figure 9, e.g., $-\text{CH} \bullet -\text{CH} = \text{CH}-$) will be resonance-stabilized. However, for saturated polymers, including XLPE and EPR, this step is thermodynamically disfavored [25]. As the termination steps in BAS (Figure 9) are in the form of reactive chain site combination, crosslinking and consequently degradation may occur. Under some conditions, peroxy termination instead of peroxy transfer can dominate [25]. Another form of termination is disproportionation, which does not create a crosslinking C – C bond and is shown in Figure 10 for ethylene radicals.

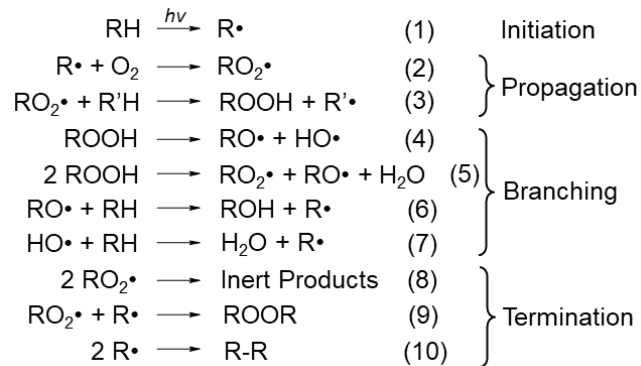


Figure 9. Basic autoxidation scheme (BAS) for polymers.



Figure 10. Disproportion of two PE radical chains [17].

Chain scission does not terminate a living radical but occurs during propagation and branching. For polyolefins in oxidative degradation, the reactions portrayed in Figure 11 contribute to scission of a polymer backbone [29]. Chain scission creates dangling chain ends that can fold themselves into crystalline lamellae.

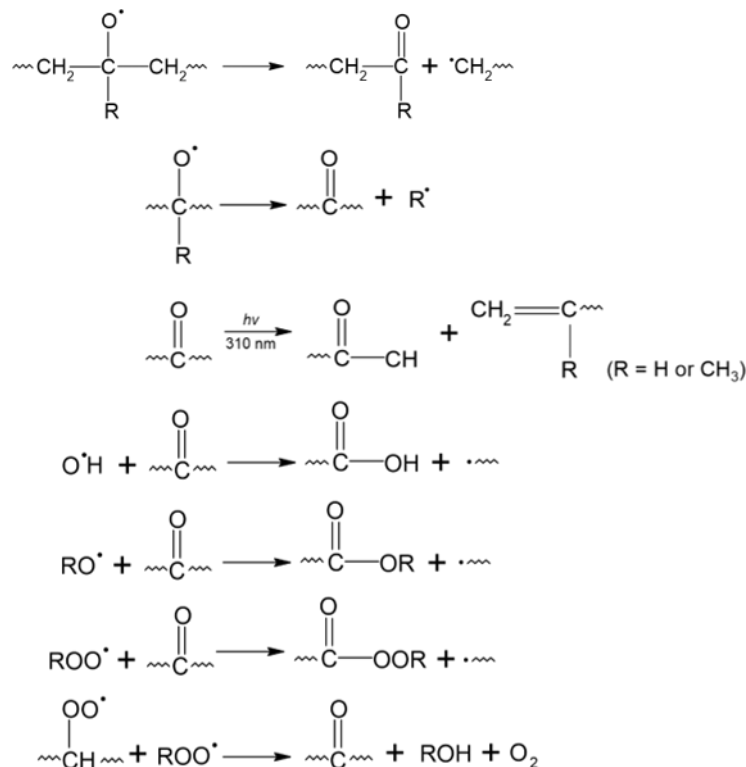


Figure 11. Scission of polyolefin backbone during photooxidation [29].

3.2 Effect of Degradation on Mechanical Properties

Oxidative degradation affects the macromolecular skeleton of a polymer through chain scission and crosslinking, causing deterioration in polymer mechanical properties. For semicrystalline polymers such as PE and polypropylene (PP), chain scission induced embrittlement is commonly attributed to a recrystallization process [30,31]. Chain scission may occur in the amorphous phase, where broken chains have high mobility and tend to crystallize, causing thickening of lamellae and decrease in interlamellar spacing [30,31]. Random chain scission can also break tie molecules (transition region molecules between the ordered crystallites and the disordered amorphous regions of a semi-crystalline polymer) [30]. When a polymer material is stretched, lamellae tilt to align with the drawing direction and split into fragments that are connected by tie molecules. The amorphous interlamellar layer allows dissipation of energy through molecular relaxation when the material is subjected to external force. This explains why polymers exhibit plastic deformation above their yield point. Thinning of interlamellar regions and breaking of tie molecules may lead to a transition from plastic and ductile behavior to brittle behavior of the polymer material. The scission-induced recrystallization mechanism can also explain embrittlement of thermally

aged XLPE. As shown in Figure 12, it was reported that an XLPE film aged at 120 °C exhibited a decrease in ductility (characterized by EAB), along with an increase in crystallinity and a decrease in crosslink density (gel fraction), indicators of chain scission [32]. The stress-strain curves of the XLPE film and an unfilled EPR film evolved differently with thermal aging at 120 °C [32]. XLPE was featured with truncation of the strain-hardening and plastic regimes, consistent with a ductile-to-brittle change (see Figure 12c) [32,33]. The unfilled EPR also showed a reduction in crosslink density, indicating chain scission during thermal aging, but modulus and yield stress decreased (see Figure 12d) [32] as the unfilled EPR was softened rather than embrittled as the network relaxed.

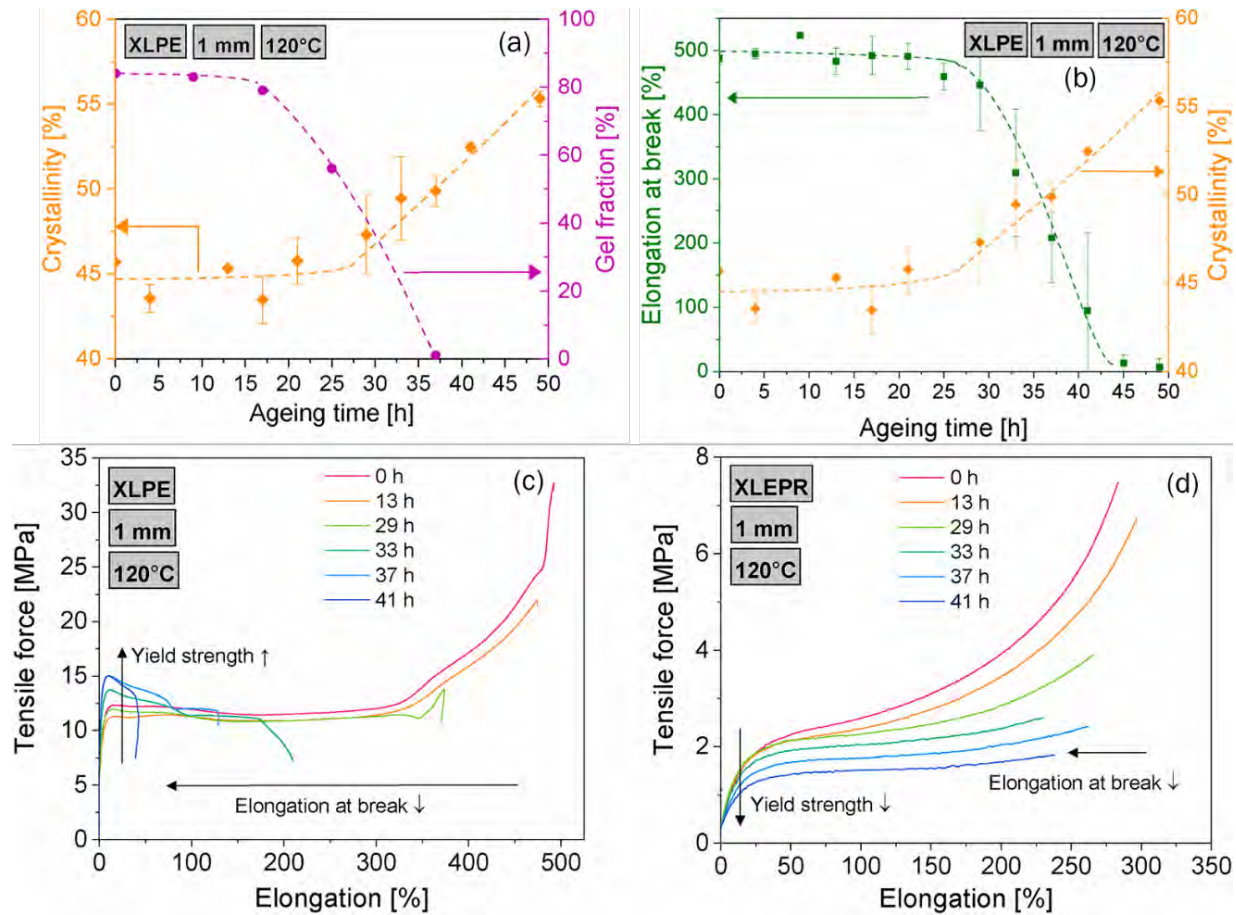


Figure 12. (a)(b) Material properties of an XLPE film changing with aging time at 120 °C. Tensile stress-strain curves of (c) XLPE and (d) EPR films aged at 120 °C for up to 41 hours [32].

In general, chain scission induces embrittlement in XLPE and other semi-crystalline polymers through a recrystallization mechanism. For elastomers such as unfilled EPR, chain scission leads to softening and liquefaction as the crosslink density decreases. Chain scission during photodegradation is limited to external surfaces for XLPE and both ethylene propylene types, whereas the core sections experience less chain scission as the radicals not involved in propagation are annihilated by combination in favor of crosslinking. The existence of antioxidants in a formulation can either scavenge peroxy radicals formed in propagation or convert hydroperoxides into non-radical products. Both types of antioxidant function can effectively prohibit chain scission and retard embrittlement onset. An induction period is observed for commercial polymers before significant oxidation and embrittlement happens [34]. However, embrittlement alone does not necessarily lead to insulation failure; external forces such as tension at the outer radius of bent cables or fatigue due to cyclic loading are primary causes of embrittled cable cracking as shown in Figure 13.

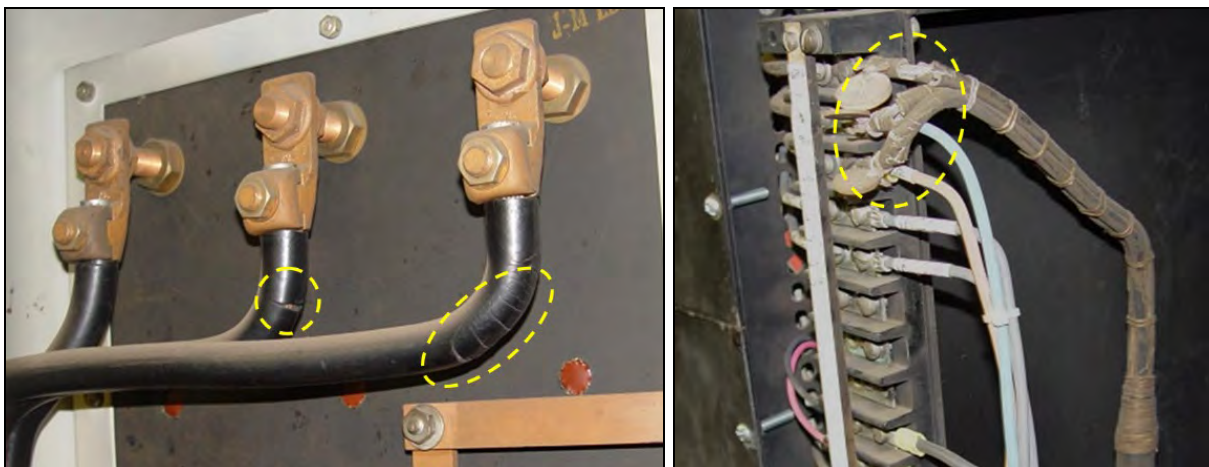


Figure 13. Cracking of polymer jacket and insulation in bend regions as circled in yellow. Photo courtesy: EPRI – cable harvesting guide, <https://cableharvest.epri.com/index.html> (registration required).

3.3 Effect of Degradation on Insulation Function

Loss of dielectric function may occur through embrittlement as discussed above but is often initiated by charge generation near impurities, such as inclusions in the formulation, degradation products, voids, defects, and moisture. Moisture degradation is of particular concern for submerged and/or underground MV cables. Charge accumulation can be identified by changes in dielectric properties, such as an increase in dissipation factor (Tan Delta) or a decrease in insulation resistance. A list of testable quantities related to cable insulation dielectric status can be found in IEEE Std 400 [35], the EPRI handbook for MV insulations [10] and the NEETRAC Cable Diagnostic Focused Initiative [36]. Techniques to measure electrical properties are also listed in regulatory guide (RG) 1.218, “Condition Monitoring Techniques for Electric Cables Used in Nuclear Power Plants”.

Dielectric stress is a greater environmental concern for MV cables than it is for LV cables due to greater electrical fields applied to MV insulation in terms of potential per insulation thickness (V/mil). Dielectric breakdown due to charge generation does not occur immediately in MV cable insulations, but is a slow process accompanied by growth of water trees. Water trees are dendritic microcavities resulting from electro-oxidation of a hydrophobic polymer to a substantially more hydrophilic state. Condensation of moisture in the hydrophilic electro-oxidized region gives rise to self-propagating tracks manifesting as water trees [37]. A review by Boggs and Xu compares the mechanisms of water tree generation in XLPE and EPR insulations [37]. A chemical potential greater than approximately 1 eV was estimated as the driving force for electro-oxidation. In addition, chemical potential was understood to vary with conductivity as illustrated in Figure 14. As XLPE has a low filler content and a low ion concentration, any ionic impurity such as cavities, particulates, cracks, etc., will increase the chemical potential and initiate a water tree. Efforts have been made to make tree-retardant XLPE (TR-XLPE) by decreasing hydrophobicity with tree-retardant additives. Compared to XLPE, EPR has more ionic content due to an increased amount of inorganic filler. The filler may generate a higher dielectric loss but may also contribute to EPR being inherently resistant to water treeing [37]. Since EPR operates on the right side of Figure 14 (higher conductivity than XLPE), common impurities do not create sufficient chemical potential to initiate water trees in EPR [37]. However, catalyst residues such as iron oxides and vanadium compounds can reduce the activation energy for electro-oxidation and become the initiation sites of water trees in EPR [37].

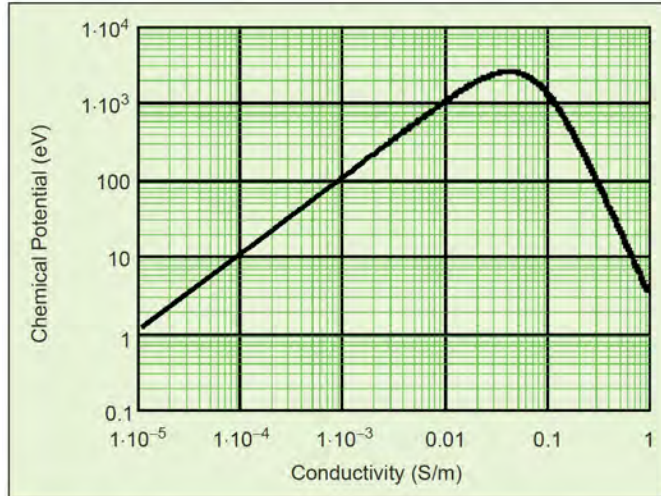


Figure 14. Chemical potential as a function of conductivity [37].

When growing water trees can no longer contain the voltage stress, an electric tree may form [38]. Time dependent growth and expansion of water trees can significantly reduce the useful life of electrical cables. Water and electrical treeing are not the only factors responsible for failure of polymeric insulation in electrical cables exposed to moisture. Failure can occur through a combination of complex mechanisms, such as partial discharge, thermo-mechanical stresses, etc.

4. Cable Aging in Qualification

Due to the inherent susceptibility of materials to experience degradation and to promote reliably safe function in NPPs, Class 1E electrical equipment, including cables, must conform to established industry performance standards as discussed in Section 4.1 and below. Generally, these standards require cable manufacturers to ensure products maintain performance requirements throughout their design life, even after design-basis accident events (DBA). In many cases, this process requires accelerated aging of the components (e.g., applying the Arrhenius method) using either thermal, radiation, or a combination of stressors, to simulate the accumulated stress of their qualified life followed by subjection of the pre-aged components to a LOCA exposure simulation. Components that successfully perform following this process are considered to be EQ. Most currently installed EQ cables have been qualified to a lifetime of at least 40 years, consistent the license period of the NPP.

4.1 Qualification Standards

NPP electrical cables are usually qualified following procedures in IEEE Standard (Std) 383 [39–41]. Type tests are the preferred method for qualification and are used to demonstrate that the cables can meet performance requirements under service conditions including normal and design basis event (DBE) environments [39]. The IEEE Std 383 supplements IEEE Std 323 which describes general guidelines and basic requirements for Class 1E equipment qualification. Versions of the applicable standards are shown in Table 3 where the four-digit number after dash “-” represents the release year. Selected versions of IEEE Std 323 and IEEE Std 383 have been endorsed by NRC in regulatory guides (RG), including:

- RG 1.89, “Environmental Qualification of Certain Electric Equipment Important to Safety for Nuclear Power Plants”;
- RG 1.131, “Qualification Tests of Electric Cables, Field Splices, and Connections for Light-Water-Cooled Nuclear Power Plants (for Comment)” (withdrawn);

- RG 1.211, “Qualification of Safety-Related Cables and Field Splices for Nuclear Power Plants”.

Table 3. IEEE Std 323 and IEEE Std 383 releases and endorsements by the NRC.

Standards	Endorsement and applicability
IEEE 323-1971, trial-use [42]	Applies to NPPs with construction permit prior to July 1, 1974, per NUREG-0588
IEEE 323-1974 [43]	Endorsed in RG 1.89, Rev 0, November 1974, and in RG 1.89, Rev 1, June 1984
IEEE 323-1983 [44]	Not endorsed
IEEE 323-2003 [45]	Not endorsed
IEEE/IEC 60780-323-2016 [46]	Endorsed in RG 1.89, Rev 2, April 2023
IEEE 383-1974 [39]	Endorsed in RG 1.131, Rev 0, August 1977, for comment (RG 1.131 is withdrawn in April 2009)
IEEE 383-2003 [40]	Endorsed in RG 1.211, Rev 0, April 2009
IEEE 383-2015 [41]	Not endorsed

Considering the construction permit issue year for NPPs in need of SLR, the IEEE standards relevant to the historical qualification of those NPPs are listed below.

- IEEE Std 323-1971, “IEEE Trial-Use Standard: General Guide for Qualifying Class 1 Electric Equipment for Nuclear Power Generating Stations” [42]. Note that aging was not listed as a part of type test procedure.
- IEEE Std 323-1974, “IEEE Standard for Qualifying Class 1E Equipment for Nuclear Power Generating Stations” [43]. Section 6.3.2 in the standard lists aging as a step in the type test procedure to simulate the expected end-of-qualified-life condition. Appendix A2 suggested the following aging sequence: (i) aging, including but not limited to accelerated thermal aging, (ii) radiation, and (iii) vibration. Aged equipment should be operated while exposed to DBE and safety functions monitored.
- IEEE Std 383-1974, “IEEE Standard for Type Test of Class 1E Electric Cables, Field Splices, and Connections for Nuclear Power Generating Stations” [39]. The standard was more specific to type testing of cables. Aging was involved in two examples of type tests: (i) testing to qualify for normal operation and (ii) testing for operation during DBE. Procedures of these two examples are depicted in Figure 15 and Figure 16, respectively.

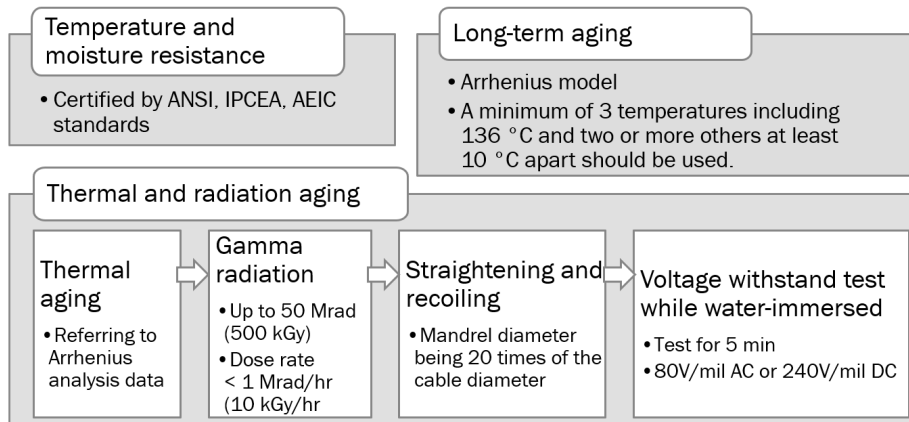


Figure 15. Type testing to qualify for normal operation described in IEEE Std 383-1974.

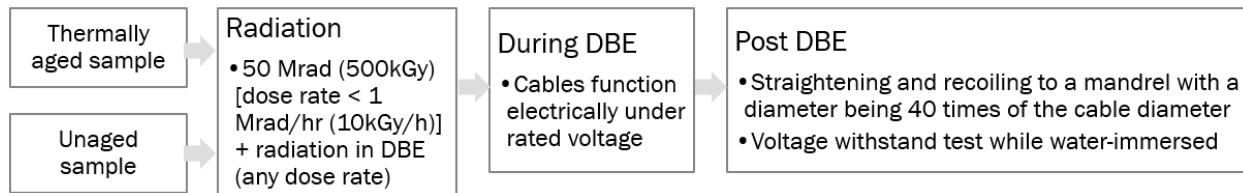


Figure 16. Type testing for operation during DBE described in IEEE Std 383-1974.

4.2 Accelerated Aging Model Assumptions

In IEEE Std 383-1974, accelerated aging is used to simulate the environmental aging of cables in service conditions over their qualified life (i.e., 40 years for the initial EQ purpose). Thermal aging is conducted using the Arrhenius model to determine an appropriate accelerated time and elevated temperature (e.g., 21 days at 150 °C) to simulate 40 years at service condition (e.g., 50 °C). Gamma radiation aging is conducted by applying a conservative estimate of the integrated dose experience by a cable in 40 years, 50 Mrad (500 kGy). Pre-aging of cables to 40-year equivalence is thus performed prior to exposing the cable to a simulated DBE such as a LOCA test to confirm that EQ cables will pass the test and perform their safety function up to the last day of their qualified life. Three major assumptions are involved in the phenomenological model, which are:

- 1) Degradation follows an Arrhenius temperature dependence throughout the entire range bracketing the service temperature and temperatures selected for accelerated aging, within which temperature range the slope of the Arrhenius plot (or the activation energy) does not change.
- 2) The same amount of degradation is imposed if the test samples are subjected to the same integrated total dose, regardless of dose rate. This assumption is often quoted as “Equal dose, equal damage” or dose rate invariancy.
- 3) Degradation caused by heat and radiation are independent and additive. If degradation (D) is a function of temperature (T) and/or radiation (R), then the assumption can be expressed in a simple mathematical expression $D(T+R) = D(T) + D(R)$.

5. Cable Aging Knowledge Gaps

NPPs in the U.S. initially received operating licenses of forty years. Most plants applying for license renewal to operate up to 60 sixty years employed re-analysis to extend the qualified life of EQ cables to 60 years based on narrowing of the abundant conservatisms employed in the original qualification. That is, service temperature and gamma exposure levels were acknowledged to be much lower in operation [e.g., < 50 °C, < 50 Mrad (500 kGy)], so that that the pre-aging process used in qualification may be reasonably considered to have imparted equivalent of 60 years rather than 40 years prior to demonstration of the ability of the cable to pass a DBE simulation. When considering subsequent license renewal, extension of plant operating licenses from 60 to 80 years, however, a closer look at the assumptions made in the original qualification process and potential issues arises in continued use of safety-related electrical cables up to 80 years was deemed necessary. As mentioned in Section 1, the NRC and the DOE assembled a group of experts on nuclear cable materials and usage to assess the status of knowledge regarding degradation in long term operation of materials in cables and cable systems. A series of cable aging knowledge gaps were identified in the report that resulted from that effort, NUREG/CR-7153, EMDA Vol. 5, related to potential concerns with the qualification process and hence with the conclusion that EQ ensures reliable operation for the entire period simulated by pre-aging. The identified knowledge gaps can be grouped into three categories of concern: (i) Situations where one or more of the model assumptions listed in Section 4.2 do not hold (also listed in Table 4); (ii) A lack of predictive model or acceleration method to study effects of moisture (see 5.9.4 in EMDA Vol. 5); and (iii) Lack of detailed

information of actual NPP environments (see 5.9.5 in EMDA Vol. 5). This section will go through the knowledge gaps in the three categories, with a summary on the phenomenon emphasized by each knowledge gap, as well as the free radical mechanisms that give rise to the phenomenon.

Table 4. Cable aging knowledge gaps originating from unsatisfied phenomenological model assumptions.

Assumption:	(1) Arrhenius temperature dependence	(2) Equal dose, equal damage	(3) $D(T+R) = D(T) + D(R)$
Corresponding knowledge gaps (sections in EMDA Vol. 5):	Non-Arrhenius behaviors at low temperatures (5.9.1); Diffusion limited oxidation (5.9.2)	Dose rate effects (5.9.2)	Inverse temperature effects (5.9.3); Synergistic effects (5.4 and 5.5)

5.1 Deviations from Arrhenius Temperature Dependence

Use of Arrhenius method to extrapolate time to failure at high temperatures (typically above 100 °C) to time to failure at the service temperature (typically between 20 °C to 50 °C) is a common practice for many applications where polymers are used. The procedure has been documented in many standards, such as ASTM G172 [47], IEEE Std 1 [48], IEEE Std 98 [49], IEEE Std 99 [50], and IEEE Std 101 [51]. Despite its widespread utility and justification based on collision theory, a kinetics theory for chemical reactions in gaseous phase, the Arrhenius method for lifetime prediction of polymers is more of a phenomenological model rather than a scientific law. It requires experimental data (i.e., “isotherms” obtained at high temperatures) and is limited to scenarios in which it is applicable (i.e., within the temperature ranges where $\log a_T$ is linear to $1/T$).

Polymers used as cable insulation are typically semicrystalline (e.g., XLPE) or rubber (e.g., EPR), as described in Section 2.3. Their mechanical durability, characterized by tensile EAB, is a good indicator of degradation and is a property relevant to its application. Therefore, Arrhenius isotherms often utilize EAB data in defining useful lifetime endpoint (e.g., EAB = 50% of initial value). As discussed in Section 3.3, a decrease in EAB, embrittlement, is a result of oxidation of alkyl radicals and subsequent chain scission-induced recrystallization. The rate-determining steps in the process are initiation (step 1 in Figure 9), typically decomposition of weak chemical bonds during thermal aging, and decomposition of hydroperoxide (step 4 in Figure 9). These two steps can be thermally activated, exhibiting Arrhenius temperature dependence. If other elementary steps are slower and determine the overall reaction rate, while not contributing to chain scission or embrittlement, deviations from linearity will be observed from the EAB-shifted Arrhenius plot.

5.1.1 Diffusion Limited Oxidation (DLO)

Within polymers, the diffusion of oxygen in the solid phase is typically slow. In oxygen deficient regions, such as the core zone of a thick piece of insulation, chain scission and consequently embrittlement are reduced as mentioned in Section 3.3, leading to a lower degradation rate than the extrapolated values. Such a diffusion limited oxidation (DLO) is observed for thick samples of insulation undergoing rapid accelerated aging at high temperatures. DLO can be observed by examining the cross-sectional profiles of degradation indicators through the sample thickness, which commonly demonstrate parabolic profiles with DLO. Common indicators suitable for microscale probing include carbonyl index measured by FTIR [52–54], surface modulus [55,56], and color change if the insulation was initially light colored [54,57]. For example, Figure 17 shows yellowing and browning of an EPR insulation after thermal aging. Discoloration of organic materials may be caused by conjugated molecular structures formed during degradation, either from polymers or additives, typically leading to the formation of carbonyl groups, which are oxidation products. In the example, circular bands of darker material can be observed for some samples aged at 150 °C and 165 °C (boxed in red in Figure 17), indicating inhomogeneous aging and less oxidation further away from the surfaces. This discoloration behavior was

quantified using the total color difference (ΔE_{ab}^*) measured between aged and unaged samples [54,57]. Note that E_{ab}^* was higher nearer to the surface, as opposed to the core zone. The same trend was observed for carbonyl index measured by micro FTIR (not shown) and oxygen concentration measured by energy dispersive X-ray spectroscopy (EDS). DLO has also been observed for XLPE insulation, in addition to EPR/EPDM.

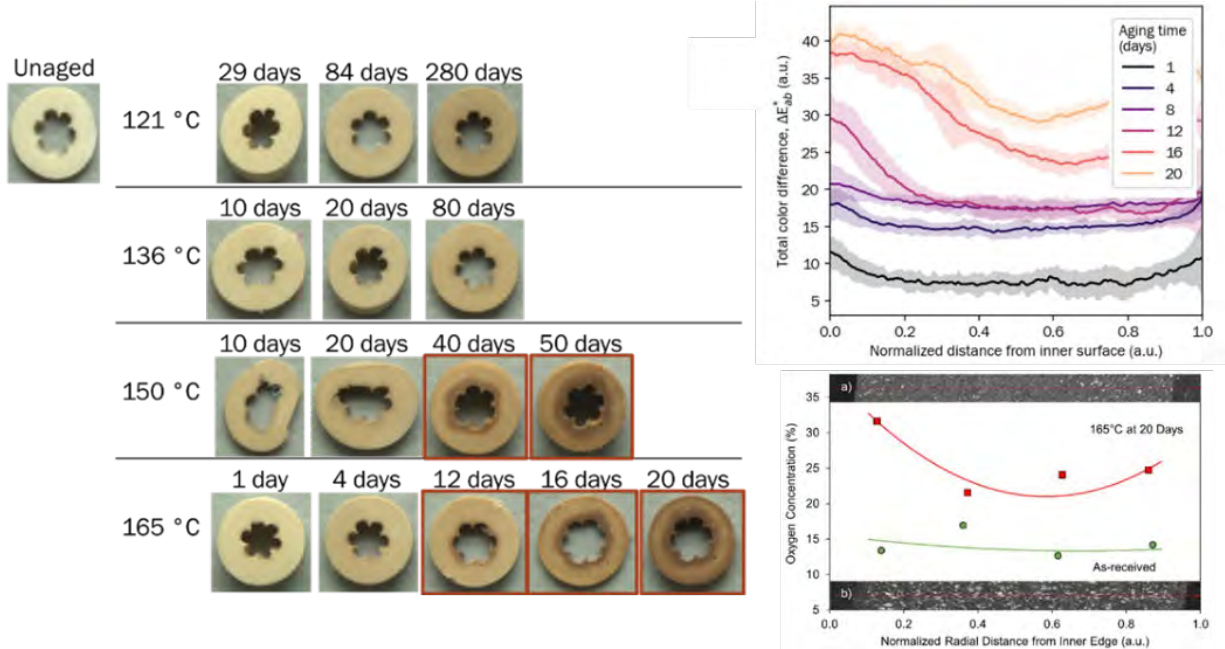


Figure 17. (Left) Color change in the cross-sections of tubular insulation specimens after thermal aging. (Top-right) Through-thickness total color difference (ΔE_{ab}^*) of EPR samples aged at 165 °C with respect to the color of unaged sample and (bottom-right) oxygen concentration measured by energy dispersive X-ray spectroscopy through thickness [57].

The historical concern has been that DLO due to extreme conditions may result in accelerated aging not being representative of service aging, nor being sufficiently conservative. If DLO shields insulation from aging at higher temperatures during accelerated aging, extrapolation of that (lack of) degradation to lower service temperatures may lead to overestimation of viable insulation service life. In general, DLO has been observed to affect lifetime prediction of cable insulation by a degree that differs by material and by performance metric [57]. Due to material variations and uncertainty in the values calculated from the indicator methods, evaluation of DLO is typically limited by the materials and conditions (temperatures) explored and in many cases may be challenging to extrapolate between material systems.

5.1.2 Non-Arrhenius Behaviors at Low Temperatures

In addition to DLO, an accelerated aging phenomena that typically occurs at high temperatures, deviation from Arrhenius temperature dependence, has also been observed at low temperature as depicted in Figure 18 [58]. Note that the figure is a conceptual demonstration and the temperature range for which linearity holds (100 °C to 150 °C) is a rough estimation for polymers in general. The actual temperature limit for Arrhenius behavior is dependent on polymer type, formulation, and test method. The non-linear deviation at low temperatures is commonly attributed to “mechanistic change” where a low-activation-energy process dominates without discussion of the specific mechanisms [59].

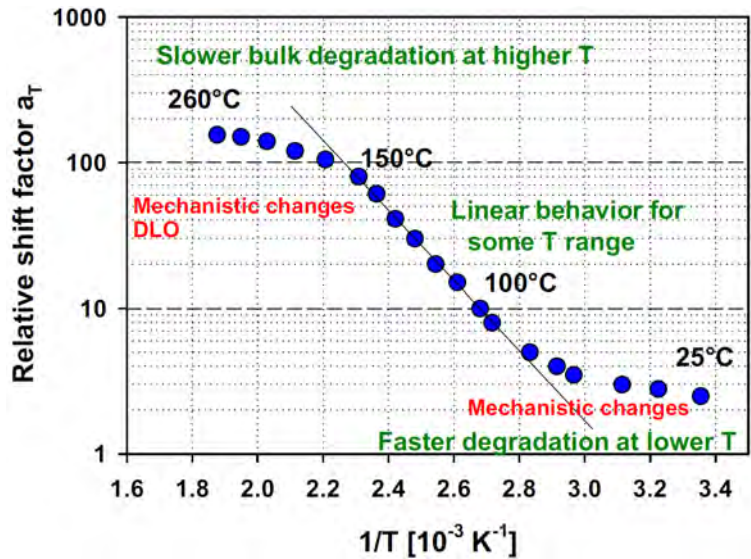


Figure 18. Deviations from Arrhenius temperature dependence above 150 °C and below 100 °C [58].

Experimental evidence of non-Arrhenius temperature dependence at low temperatures has been reported for many polymers, including PP [59], XLPE [60], EPR [60], and polychloroprene (aka neoprene) [61]. While not commonly used as insulation in U.S. nuclear cables, neoprene may be found as a jacket material, and its premature degradation could have adverse effects on cable insulation performance if it were part of a bonded jacket/insulation construction. Neoprene is known to be particularly susceptible to thermal damage, especially relative to the EPR and XLPE materials commonly used in nuclear cable insulation. An example of non-Arrhenius behavior is shown in Figure 19 for EAB isotherms of neoprene. The Arrhenius plot is shown with shift factors (a_T , characteristics of phenomenological degradation rate) obtained from the EAB isotherms, where the data points at 24 °C were measured after 24 years and 19 years [61]. A decrease in the slope is evident towards 24 °C. In addition, the shift factor $\log a_T$ from extrapolated data points (solid line in Figure 19) is lower than the actual $\log a_T$, which means the extrapolated EAB isotherm at 24 °C is located at longer time than actual, or put simply, qualified life was overestimated at 24 °C.

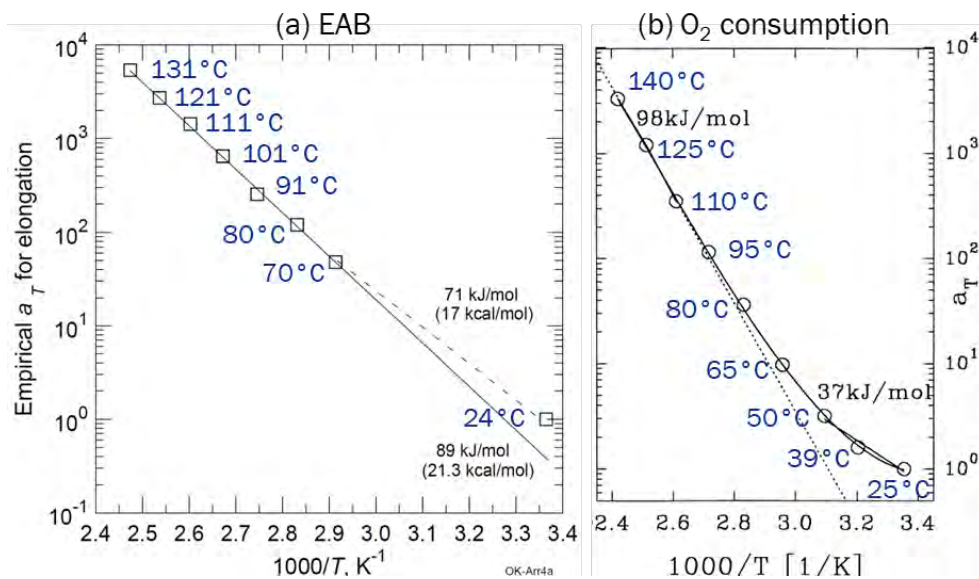


Figure 19. Deviations from Arrhenius temperature dependences evident by (a) EAB of a chlorprene rubber jacket [61] and (b) oxygen (O_2) consumption of another chlorprene rubber with fewer fillers [53].

Low-temperature mechanical data (below 50 °C) is difficult to obtain since degradation to a measurable state at this temperature can take years to decades. This is especially true when using EAB as an indicator of degradation since significant embrittlement may have a long induction time as mentioned in Section 3.3. Indicators that are more sensitive to polymer degradation, such as level of consumed oxygen, have been used to reveal degradation at low temperatures in a short time frame when EAB has yet to reflect significant changes [53,62]. For example, the same deviation as observed from the 20-year aged neoprene is shown in Figure 19 consisting of a_T obtained from oxygen consumption data [53]. At lower temperatures, the actual consumption of oxygen is faster than would be extrapolated from high-temperature data points, which implies that alkyl radicals ($R\bullet$), once generated, are more prone to be oxidized at lower temperatures and that propagation (step 2 in Figure 9) is more competitive over termination. The implication is not impossible considering that hydroperoxide products can be metastable at low temperatures. However, further study on the kinetics of the chemical and physical processes is needed to determine the “low-activation-energy” process [59].

5.1.3 Uncertainties and Variabilities

The Arrhenius method makes use of estimated activation energies (E_a) for the degradation process, which is used to predict insulation lifetimes. Uncertainties in activation energy and uncertainties in qualified cable life projection are important to decision-makers for SLR. Sources of uncertainties in E_a include but are not limited to: (i) experimental data used to construct isotherms, (ii) criteria used to shift and align isotherms, and (iii) linear regression of shift factor vs. reciprocal of temperature. Many factors can contribute to sources of uncertainty in experimental data, including shape of sample for tensile testing (dog bone vs. tubular), variation in material formulation, dispersion of additives through a series of samples, etc. In addition, the choice of degradation indicator also affects the computed E_a value as different techniques probe different characteristics of materials and may reflect different stages of aging. Current standards have adopted upper and lower confidence limits for selected service and test temperatures, such as for source (i) in IEEE Std 101-1987 [51] and NISTIR 8391 [63] and source (iii) in ASTM E2070 [64] and ASTM E1970 [65]. Uncertainty arising from source (ii) can be estimated by calculating different E_a from all applicable end points [63].

5.2 Equal Dose, Equal Damage Assumption

The second pre-aging assumption, associated with radiation aging, is “equal dose, equal damage” or dose rate invariance, $Damage(c \times Dose) = c \times Damage(Dose)$ where c is a constant. Examination of this assumption can be performed by simply plotting degradation indicators, such as EAB, against the integrated total dose (dose rate \times aging time) for different dose application rates. If EAB values collapse on the same curve, then they are dose rate invariant. Otherwise, there is a dose rate effect in the dataset. Figure 20 is a schematic presentation of a normalized EAB (e/e_0) dataset with dose rate effect present, where the samples aged at lower dose rates degrade with total dose faster than the ones aged at higher dose rates [66].

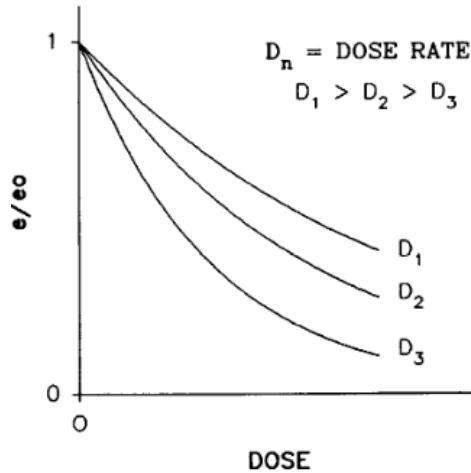


Figure 20. Illustration of dose rate effects present in an EAB dataset [66].

5.2.1 Dose Rate Effects

Dose rate effects can be explained by additional levels of alkyl radicals generated at high dose rates that do not propagate (see Section 3.2 for discussion). Reduced propagation means less chain scission-initiated embrittlement, and therefore a delayed decrease in EAB as shown in Figure 20. In other words, a higher dose rate only accelerates the initiation step (step 1 in Figure 9), which does not always accelerate the overall degradation rate or macroscopic embrittlement. At low dose rates where initiation is the rate-limiting step, faster initiation can lead to faster overall degradation, which is where the “equal dose, equal damage” assumption is valid. Since temperature is assumed to accelerate all degradation steps, the upper limit of dose rate for the “equal dose, equal damage” region increases with temperature, as illustrated in Figure 21.

The dose rate effect has been observed for XLPE samples above approximately 250 Gy/h (25 Mrad/h), but not for the EPDM samples up to 2.5 kGy/h (0.25 Mrad/h) aged at the same conditions [66,67]. The same conclusion was reached in a more recent study within an LWRS project [68], where the dose rate effect was clearly observed for XLPE but not for EPDM according to EAB results. The report also included carbonyl index, discoloration, density, and indentation datasets but these chemical measurements did not differentiate the dose rate effects. Dose rate effects have been reported for LDPE [69,70] and PVC [71], but these materials are rarely found in U.S. nuclear cable constructions. Elastomers such as EPDM, EPR, silicon rubber and the fluoroelastomer Viton seem to be less susceptible to dose rate effects [66,67,72]. A saturation in oxidation rate (correlated to radical propagation rate according to step 2 in Figure 9) was observed at high dose rates for a Viton rubber, supporting the assumption that dose rate effects are due to limited chain propagation [73].

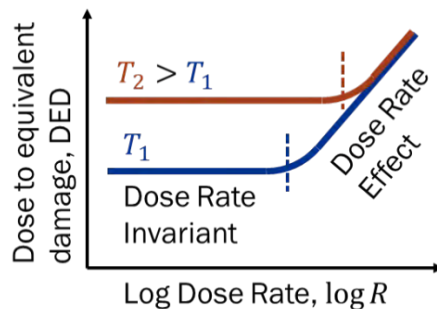


Figure 21. Illustration of the onset dose rate (dashed lines) for dose rate effect at different temperatures.

5.3 Synergism of Thermal and Radiation Aging

The third assumption listed in Table 4 is that degradation due to thermal and radiation stressors are additive, or that there are no synergistic effects. This can be dissected into two subordinate assumptions: (i) degradation caused by thermal-only and radiation-only aging are equivalent to the degradation when heat and radiation are both present, and (ii) the sequence of thermal-only and radiation-only aging is inconsequential. In EMDA Vol. 5, it was stated that “degradation is more severe in concurrent aging and least severe in sequential aging where the thermal aging is carried out before radiation aging” which raises concerns about the historical EQ process being sufficiently conservative. The conclusions in EMDA Vol. 5 may be assumed to be based on studies described in NUREG/CR-3629 [74] and NUREG/CR-3538 [75].

5.3.1 Synergism of Thermal and Radiation Aging

Neither the third assumption listed in Table 4 (thermal and radiation aging additive) or the assumption in EMDA Vol.5 (concurrent aging more severe) are supported by the EAB data shown in Figure 22 for XLPE and EPDM [76]. In that work, three sets of samples were exposed to one of three aging conditions: (1) “T/R”: simultaneous aging at 150 °C and 300 Gy/h (30 Mrad/h), (2) “T+R”: sequential aging of thermal-only at 150 °C followed by radiation-only at 300 Gy/h (30 Mrad/h) and room temperature (26 °C), and (3) “R+T”: sequential aging with reversed order compared to T+R. Note: the temperature and dose rates explored in that work were selected based on experimental constraints rather than as an attempt to directly mirror conditions used in historical qualification processes. In the EAB results, XLPE under the T+R (thermal then radiation) condition was observed to degrade fastest, whereas EPDM degraded fastest under the reversed order, R+T (radiation then thermal) condition. A significant mass loss for EPDM was found in the second, thermal aging step comparing the mass change data in Figure 22 for “R” and “R+T” scenarios. The extra mass loss of EPDM could be explained by thermal decomposition of metastable hydroperoxides produced in the former radiation step, leading to excessive chain scission and formation of volatile species in the second, thermal aging step [77]. However, the hydroperoxide decomposition assumption is not applicable for XLPE. The overall synergistic phenomenon of XLPE could be a convoluted result of multiple chemical and physical processes occurring simultaneously during aging including competition between chain scission (favored by propagation/oxidation) and crosslinking (favored by termination), recrystallization of broken chains, annealing (or crystal perfection) at high temperatures, and the decomposition of metastable hydroperoxides and ketones in the subsequent aging [77,78]. The effects of chain scission are also different for XLPE (embrittlement) and for unfilled EPR (liquefaction and loss of integrity) as mentioned in Section 3.3. In fact, EAB responses of two EPRs reported in NUREG/CR-3629 (see Figure 23) showed opposite trends to that of EPDM, but similar characteristics to that of XLPE in Figure 22 [74]. In Figure 23, EPR 1, EPR 2, and cross-linked polyolefin (XLPO) 2 all exhibited fastest degradation during the radiation aging step that cannot be explained by the hydroperoxide decomposition mechanism solely. Experimental investigation and kinetics modeling are needed to further elucidate the mechanism of synergistic effects, especially for XLPE.

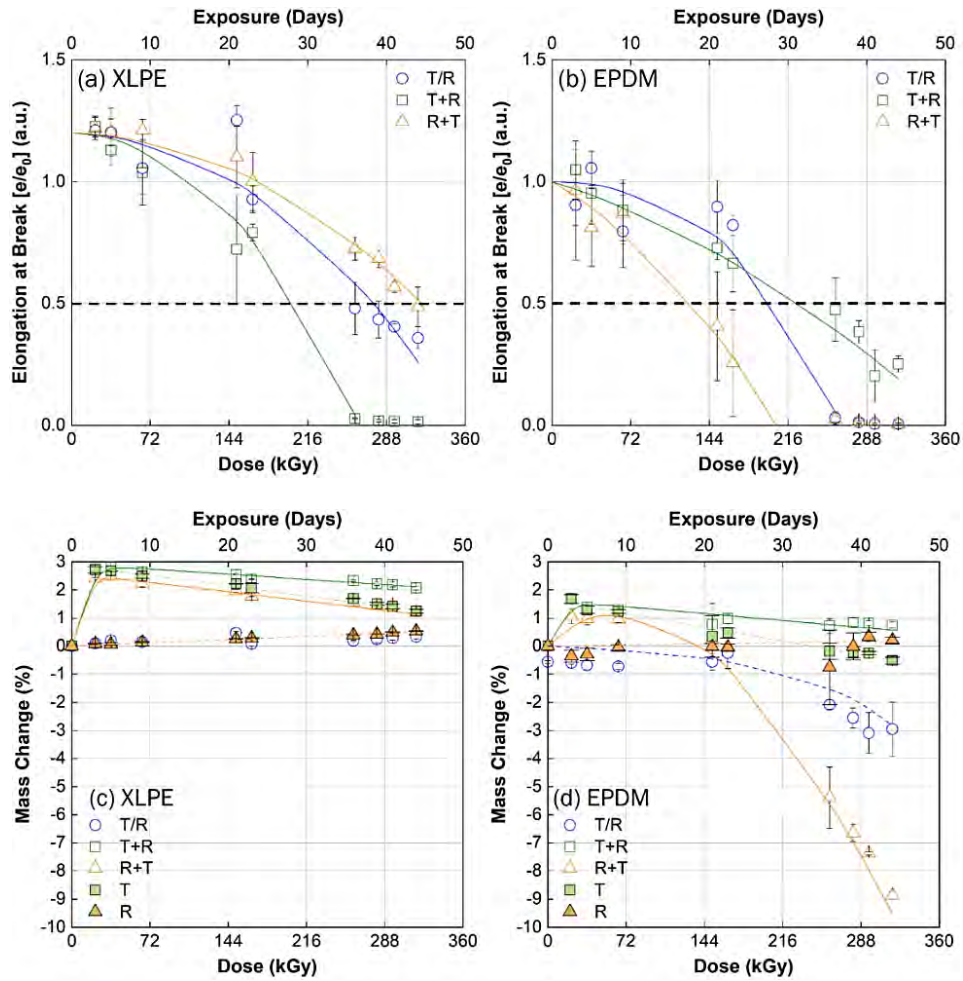


Figure 22. Normalized EAB with total dose for (a) XLPE and (b) EPDM aged at three conditions: T/R: 150 °C and 300 Gy/h (30 Mrad/h) simultaneously, T+R: thermal-only aging at 150 °C, followed by radiation aging at 300 Gy/h (30 Mrad/h) and room temperature (26 °C), and R+T: the reverse of T+R. Mass change relative to the unaged samples for (c) XLPE and (d) EPDM after the same aging conditions [76].

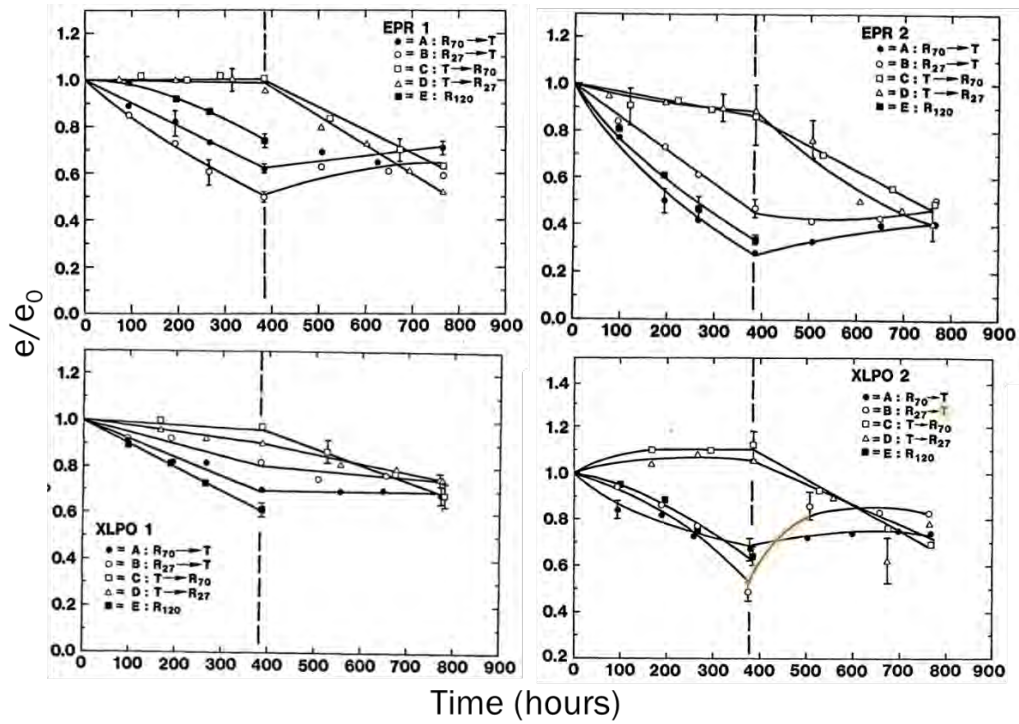


Figure 23. Normalized EAB with respect to aging time in sequential and simultaneous aging conditions: “T” means thermal aging at 120 °C and “R” refers to radiation aging at 650 Gy/h (65 Mrad/h). The number beside “R” refers to the temperature in °C during radiation aging. The highlighted datapoints showed an increase in EAB [74].

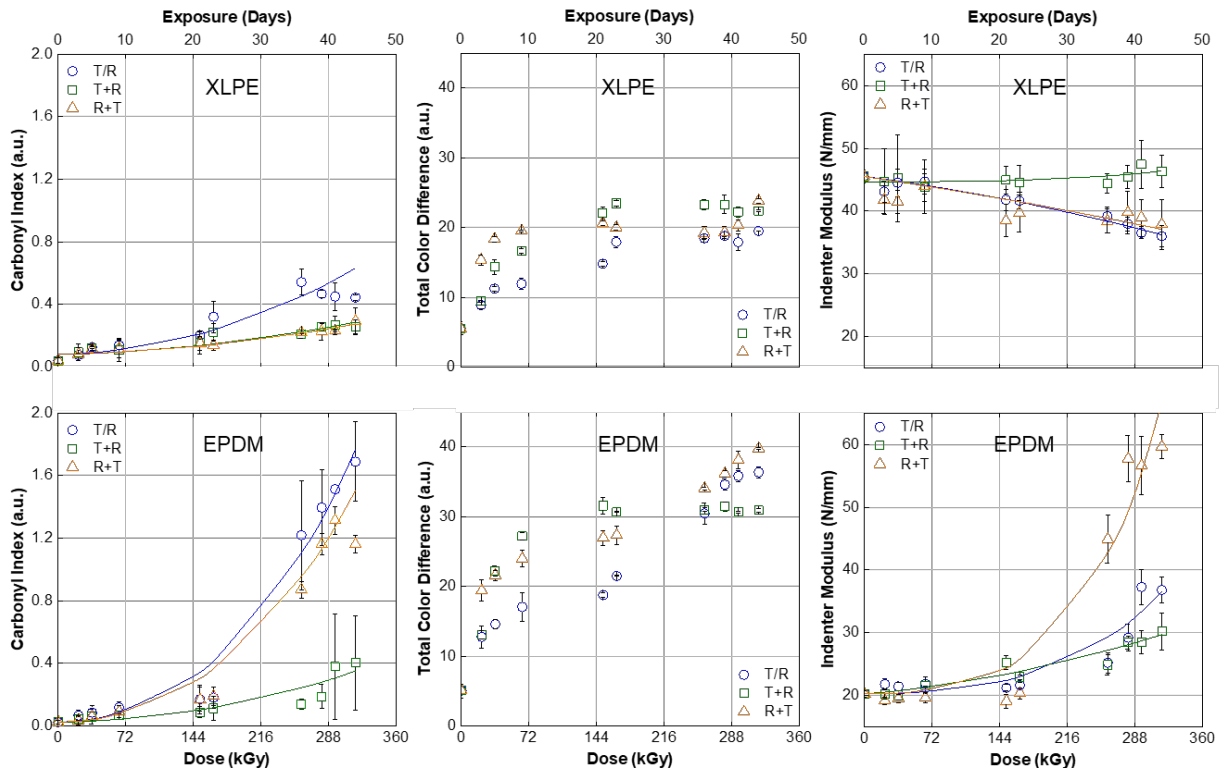


Figure 24. Carbonyl index, total color difference and indentation modulus of XLPE and EPDM subjected to simultaneous (T/R), sequential (T+R) and reversed simultaneous (R+T) aging. The temperatures and dose rates are the same as in Figure 22 [76].

Other degradation indicators were also studied in the report [76], including carbonyl index, total color difference, and indentation modulus as plotted in Figure 24. For XLPE, these additional datasets together with mass change (see Figure 22) did not show faster degradation in the T+R scenario as observed in the EAB dataset. Thus, the synergistic effect of XLPE in that work seems to be only relevant to mechanical embrittlement [76]. As shown in Figure 22, the mass gain during simultaneous aging (T/R) is very close to the mass gain during radiation-only aging (R), implying that radiation might be the dominant factor. On the other hand, for EPDM, all measurements including EAB were found to produce the same conclusion, namely R+T was the most degradative aging condition for EPDM, within expectations from the hydroperoxide decomposition assumption.

During EQ of cables, thermally aged samples are subjected to 50 Mrad (500 kGy) radiation before DBE, which represents the most severe aging scenario for XLPE (T+R) and injects conservatism in the current EQ procedure. For EPR/EPDM, the EAB responses from two studies (Figure 22 and Figure 23) showed an opposite trend and whether the EQ procedure is conservative may depend on the formulation and values of dose rates and temperatures. However, since the decrease in EAB correlates well with other data for EPMD, multiple measurements including some suitable for online monitoring may facilitate decision making in cable aging management.

5.3.2 Inverse Temperature Effects (ITE)

So-called “inverse temperature effects” (ITE) refer to the counter-intuitive scenario in which polymer degradation, in the presence of radiation, proceeds more rapidly at lower temperatures than at higher temperatures.

ITE have been reported for XLPO materials irradiated at room temperature (22 °C) but were not observed above 60 °C [79,80]. However, embrittlement of XLPO at room temperature was recoverable upon subsequent heating (annealing) as shown in Figure 25; the same recovery was also observed for XLPO 2 as highlighted in Figure 23. In addition, both density and gel fraction were reported to show ITE for XLPO [79,80]. In an LWRS report [81], systematic studies were conducted and focused on an XLPE material that clearly exhibited ITE as shown in Figure 26 and an EPDM material that did not show significant ITE. However, non-Arrhenius behavior as described in Section 5.1 was observed for EPDM in the report. From the LWRS report [81], ITE were only observed in EAB datasets for XLPE and not for other degradation metrics as shown in Figure 27.

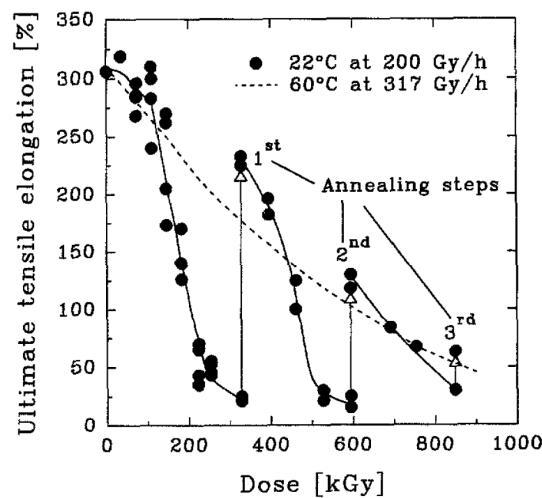


Figure 25. Recovery of EAB upon annealing at 140 °C for 24 h, after room temperature (22 °C) radiation aging at 200 Gy/h (20 Mrad/h) [79,80].

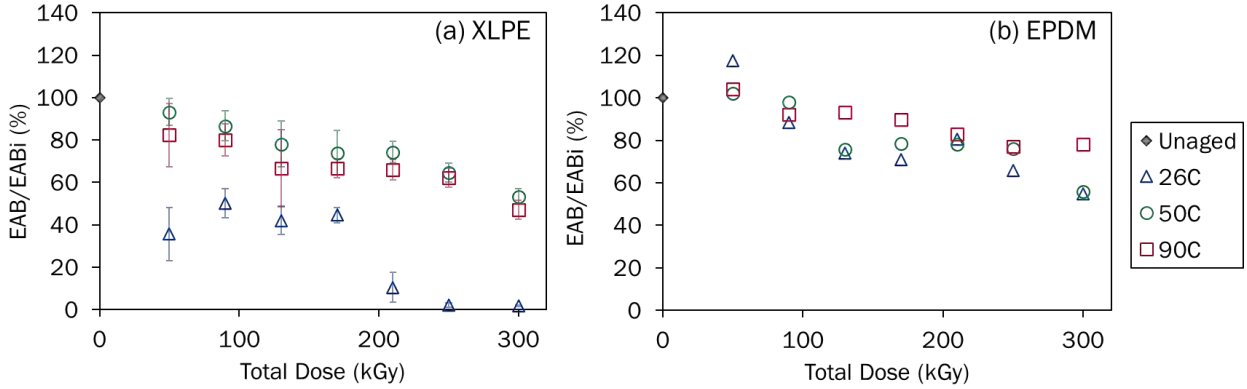


Figure 26. Normalized EAB of (a) XLPE and (b) EPDM aged at 100 Gy/h (10 Mrad/h) and 26 °C, 50 °C, 90 °C [81].

ITE of XLPE are consistent with the fact that T+R (thermal then radiation aging) poses the most severe degradation on XLPE as shown in Figure 22, as radiation was the last step before tensile testing and no crystal annealing would be performed to recover embrittlement resistance. ITE also explain the fast degradation during radiation observed in Figure 23 and the mild (for EPR 1 and EPR 2) to more obvious (for XLPO 2) recoveries in the subsequent thermal aging step. It may be deduced that EPR 1 and EPR 2 have high ethylene content such that they form substantial crystalline phases. Based upon findings in previous work, it is hypothesized that the mechanisms for ITE are related to recrystallization induced embrittlement for XLPE and for some semi-crystalline EPR, and the re-initiation of metastable species for EPDM.

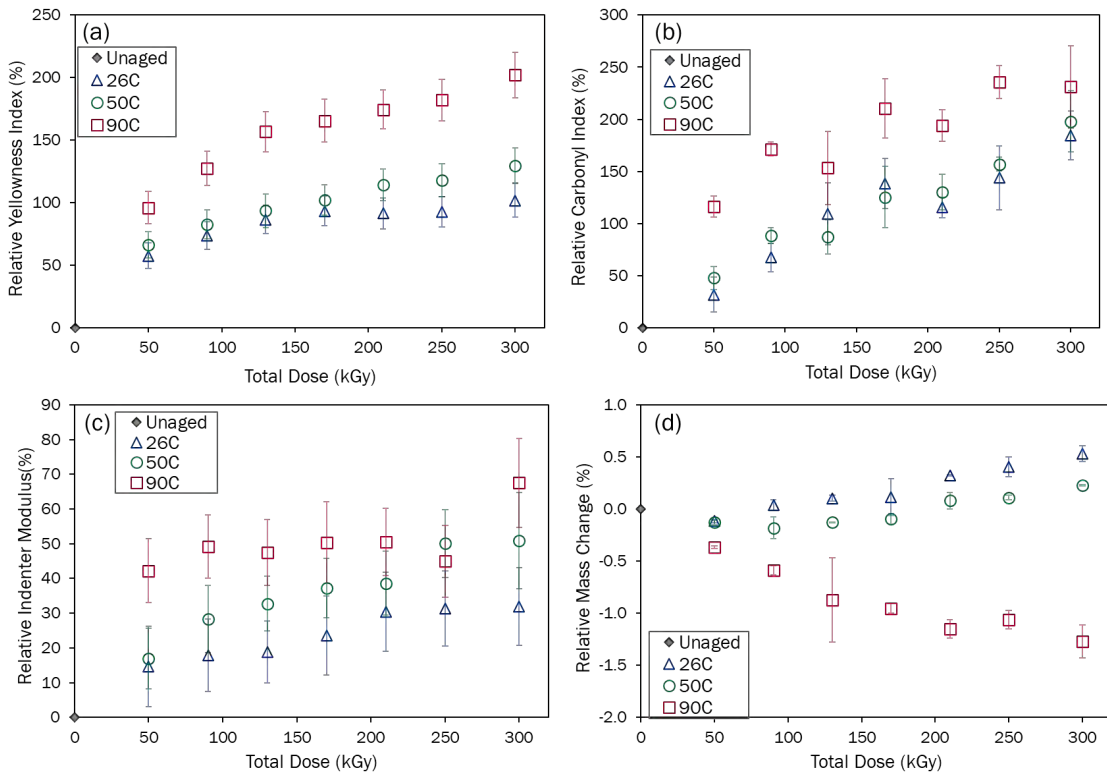


Figure 27. Normalized (a) yellowness index, (b) carbonyl index, (c) indenter modulus and (d) mass change of XLPE aged at 100 Gy/h (10 Mrad/h) and 26 °C, 50 °C, 90 °C [81].

The results of previous work do not support the conclusion that ITE in cable qualification necessarily exclude safe continued use of existing cables. Inverse temperature effects were found to differ based on insulation material and on property measured. The practice of subjecting cables to thermal aging followed by radiation aging at room temperature in qualification appears to be a conservative scenario for materials exhibiting ITE. Ongoing non-destructive cable system condition monitoring is encouraged to support repair and replace decisions for continued safe and effective use of electrical cables in long term operation.

5.4 Moisture Effects

While thermal and radiation aging mainly affect mechanical properties, moisture is more relevant to dielectric function, which is a concern for MV cables, especially underground and/or submerged cables. The mechanism of loss of dielectric function involving moisture and electrical field have been discussed in Section 3.4. Unlike thermal and radiation aging that follow a free radical degradation mechanism such as BAS (see Figure 9) and can be approximately described by phenomenological models, the effect of moisture has not been captured by a widely accepted model with sufficient predictive power. In SAND-2015-1794 [14], a thorough literature review was performed on the mechanism of moisture-related aging of MV cables and on relevant condition monitoring techniques. The review concluded that “there is no uniformly accepted methodology, mechanistic model, or empirical model that can predict lifetimes or performance changes as a function of time [for submerged cable degradation]” [14], and that “there is no simple path forward to obtain a more comprehensive model due to the complexity [of a variety of environmental stressors involving] water, ions, voltage, temperature and other factors” [14].

A Nuclear Energy University Program (NEUP) project led by University of Minnesota Duluth (UMD) focused on a “mechanistic, predictive understanding of aqueous impact on ageing” of MV and LV cables [82]. Many topics related to a mechanistic understanding were separately studied with the following results:

- The water vapor permeability of PE films increased as it was oxidized;
- PE films doped with gold nanoparticles (AuNP) were synthesized with the assumption that AuNP would occupy voids during dielectric breakdown and help visualize pore structures;
- PP and PE samples aged at dry, submerged, and cyclic dry-rewetting conditions in water and ionic salt solutions, all at 90 °C, showed no significant differences in terms of carbonyl index, elastic modulus, and yield strength;
- Capacitance increased with water tree length gradually, while resistance decreased rapidly as the water tree tip approached the conductor;
- No increase in partial discharge was detected during a 2-year aging of harvested MV power cables at 60 Hz, 90 °C, and elevated voltages (30 kV for XLPE and 12 kV for EPR cables).

Research conducted by EPRI concluded that water trees are one of the leading degradation mechanisms that contribute to the loss of dielectric insulation strength in MV cable materials in wet or submerged environments. The electrochemical reactions are caused by the combined effect of the presence of water and high electrical stress. The relative importance of these causal stressors can vary among cable installations and are not specifically measured in most cases. Records of cable failures provided by nuclear plant operators confirm the reliability concern for MV cables in wet or submerged environments and served as a basis for developing the EPRI test program. Practical management of this kind of damage is based on performance tests. EPRI dissipation factor or Tan Delta ($\tan\delta$) testing guidelines and acceptance criteria have been adopted by most NPP operators as the primary tool for condition monitoring of MV cables in wet or submerged environments. EPRI collected member data from 2009 to 2012 to analyze and validate the EPRI-developed acceptance criteria guidelines [83–86] and to support forensic research on causes of insulation degradation and failure. The guidelines advise Tan Delta

testing every 6 years if test values are in the “good” or green range and every 2 years if test values fall into the “further study” or yellow range. Guideline values are insulation material specific and may not be available for all cable insulation materials. PNNL performed a statistical review the EPRI reports and the associated data with specific plant information redacted. The PNNL analysis implied that the EPRI guideline thresholds are appropriate, as documented in the PNNL-28542-1 report [87].

5.5 Actual NPP Environments

As part of their long-term operations (LTO) program, EPRI collected cable environmental service condition data during normal plant operations in both pressurized water reactor (PWR) and boiling water reactor (BWR) environments. Survey results are presented in EPRI-3002000816 [88] and EPRI-3002010404 [89]. Both reports confirmed operating conditions for both temperature and radiation being lower than design values [50 Mrad (500 kGy) for a total of 40 years, 49 °C in containment, 40 °C in auxiliary building]. The EPRI-3002010404 report also points out that LV I&C cables can be more susceptible to degradation in high radiation and ambient environments, consistent with the inverse temperature effects discussed in Section 5.3.2.

6. Path Forward on EMDA Vol. 5 Knowledge Gaps

Knowledge gaps identified in the EMDA Vol. 5 represent concerns that the assumptions made in 40-year environmental qualification of cables may be weak, that the pre-aging of cables prior to LOCA testing may have represented less than 40-year equivalence, and that consequently the EQ process may not be conservative and thereby overpredict cable useful lifetime. While cable failures have been observed to be relatively few in the first 40-60 years of plant operation, the concern is that lack of conservatism in the 40-year qualification is a more serious issue in licensing up to 80 years. Subsequent research by DOE and others in the years following publication of the EMDA Vol. 5, as reviewed herein, found that the Arrhenius and equal dose/equal damage assumptions of thermal and radiation aging behavior on which the historical qualification process was based hold for some relevant cable materials, accelerated aging conditions, and performance metrics and do not hold for others. While the pre-aging process appears to be not conservative in some cases, it appeared to be conservative in many others.

Three approaches to maintain confidence in the continued reliable performance of existing nuclear electrical cables in long term operation are: 1) advance comprehensive cable condition monitoring programs using existing and newly developed tools to inform decisions to repair, replace, or retain cables as needed, 2) pursue additional aging studies and the characterization of harvested materials for greater understanding of nuclear cable insulation degradation in the nuclear plant environment, and 3) utilize modeling and simulation to predict cable performance from material measures. Targeted materials aging studies, modeling and simulation of material composition/exposure/performance relationships, and evaluation of harvested cables will support use of a testing-based approach for cable aging management in existing light water reactors.

6.1 Advanced Aging Studies

As identified in the EMDA Vol. 5, correlation of accelerated aging to long term service aging is often challenged by differences in degradation mechanisms in the two scenarios. Breakdown of polymer structure at high temperatures and high dose rates in a short period of time can be different than the breakdown that occurs under the relatively mild conditions that contribute to aging over many decades in an NPP. Better predictive understanding of the service aging of materials could be obtained through accelerated aging at milder conditions closer to service conditions, more accurate measurement of environmental conditions at cable service locations, and harvesting of aged cables from plants for validation of actual service aging.

6.1.1 Improved Accelerated Aging

More representative accelerated aging means better replicating the in-service environment such as through use of lower temperatures ($< 100\text{ }^{\circ}\text{C}$), lower dose rates [$< 100\text{ Gy/h}$ (0.01 Mrad/h)], concurrent aging, etc. Milder aging conditions will result in aging that more closely resembles service aging but will dramatically increase the time to significant aging of test materials from weeks or months to years or many years. This challenge may be mitigated through use of sensitive measures of aging that enable prediction of aging curves early on the aging process. Rather than measuring a full aging curve from unaged condition to end of life in a few months at a higher temperature, an indication of aging that is sensitive over the entire aging curve might be employed to measure the first few months of a multiyear aging curve at milder temperature and then used to predict the time to endpoint without waiting until the full aging curve is complete. Oxygen consumption is a potential example of such a sensitive measure.

Although the well-established metric EAB has historically trended best with aging, especially towards the end of useful life, it often shows an “induction time” during initial degradation. As shown in Figure 19, the advantage of using oxygen consumption to reveal the deviation from Arrhenius temperature dependence at around $50\text{ }^{\circ}\text{C}$ is demonstrated. Practically, oxygen consumption can be performed within a short time near service temperatures, in a regime in which EAB is insensitive to degradation. Oxygen consumption measurement may be considered an “ideal indicator” if it sensitively and linearly trends with degradation throughout the entire insulation lifetime. If that was the case, EAB isotherms obtained from different temperatures and dose rates should be readily superimposed when plotted against the oxygen consumption measured at the same aging condition, and no empirical time-temperature or time-dose rate superposition would be needed. A few datasets in the Sandia Cable Repository of Aged Polymer Samples (SCRAPS) spreadsheet [90] reveal superposition of EAB isotherms when plotted against oxygen consumption as shown in Figure 28. Rigorous derivation and experimental verification are needed to determine how EAB is dependent on oxygen consumption and to examine if oxygen consumption can be considered an ideal indicator. In a review paper on combined radiation-thermal aging [91], the concept of “oxidation level” was proposed as the ratio of oxygen consumption divided by the total allowed oxygen consumption at failure. The oxidation level was then used to represent the state of degradation progress. Plotting EAB or any material property data against oxygen consumption as in Figure 28 is equivalent to parameterizing shift factor (a_T) as the ratio of oxygen consumption rate (φ), i.e., $a_T = \varphi_T / \varphi_{ref}$. Comparing a_T determined empirically (by shifting EAB isotherms) and a_T calculated from $\varphi_T / \varphi_{ref}$ could be a way to examine if it is valid to consider oxygen consumption as the degradation progress.

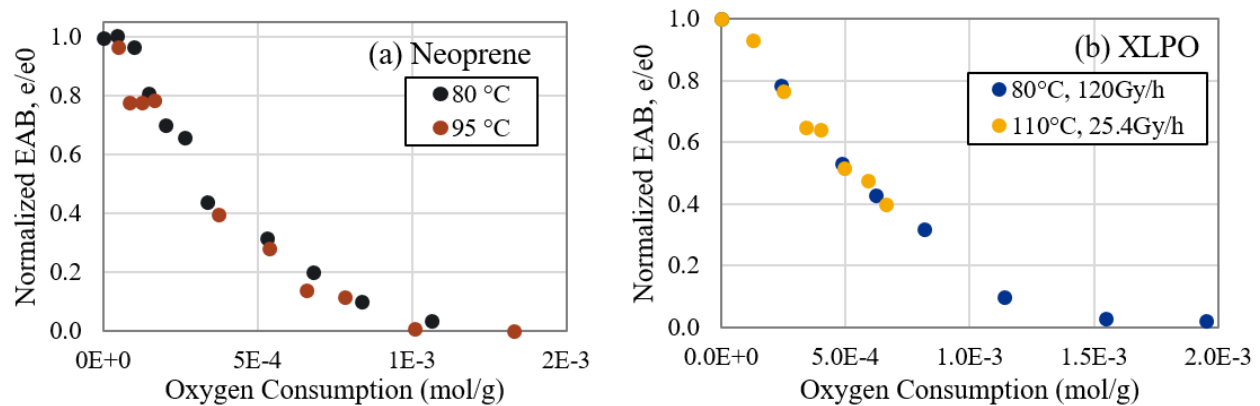


Figure 28. Superposition of normalized EAB isotherms when plotted against oxygen consumption of (a) neoprene and (b) XLPO samples. EAB data were obtained in SCRAPS with sample ID (a) “Neo-02” and (b) “XLPO-02A” [90]. Oxygen consumption data were found in published papers and reports [61,92].

Currently, experimentally measuring oxygen consumption requires measuring the mole number of oxygen before and after sealing polymer specimens in an airtight vessel, which is not readily applicable

for field testing or online monitoring. The oxygen consumption technique is limited to lab research, for example, to provide activation energy values at low temperatures. Other sensitive measures of degradation have been examined and compared to oxygen consumption results in an LWRS report [93]. Changes in mass of polymer samples, carbonyl index, and discoloration also showed decent sensitivity to early insulation degradation, but their applications have been limited [93].

Limitations to the use of sensitive measures of aging to simulate service aging at closer to service environmental conditions include unknowns regarding the intermediate or long-term aging behavior to be predicted from early signals. The weak assumptions of classical accelerated aging at more severe conditions might still exist in correlating measures of aging in mild aging curves to those in more severe condition aging curves for endpoint prediction. Additional limitations to the strategy of relying on use of more sensitive measures of aging and more representative accelerated conditions to predict cable failure include that historic cable materials of interest are in limited supply. Aging studies require time and funding, but also sufficient material to produce confident results. Most of the cables of concern in long term operation are no longer manufactured and in scarce supply for research. Furthermore, laboratory testing of representative materials cannot well predict sources cable failure such as manufacturing defects, defects from installation, workmanship issues, and degradation from unexpected adverse local environments. All of these may require in-service testing to discover.

6.1.2 Better Understanding of Cable Environments

High resolution correlation of accelerated aging to service aging to understand cable performance in long term operation depends on good understanding of plant environments. Certain environments in the plant may have elevated dose rates, elevated temperature, or moisture, while many others have mild ambient conditions. Expanded use of temperature, moisture, and dose monitors in existing plants could provide a technical basis for cable longevity expectations—providing better understanding of cable environments and validating reductions in conservatism in license renewal. Fiber-optic distributed temperature sensing, RFID tags, and wireless transmitters are examples of technologies that could be utilized for this purpose. Limitations to this approach include the cost of purchasing, installing, and monitoring sensors. Access to locations of interest and security concerns with wireless transmission are additional barriers.

6.1.3 Harvested Cables

Understanding of cable aging in actual plant service environments could be most directly informed through evaluation of cables harvested from plants following long periods in service. As cables come out of service during maintenance or following plant decommissioning, they could be used to compare actual vs. predicted changes in material performance. To be useful for expanding our understanding of in-service aging, information regarding the identity and the history of a harvested cable is essential. To avoid damage to neighboring cables in a tray, a cable taken out of service is often abandoned in place and not available to be harvested. For convenience, extracted cables are often cut into few foot lengths during removal, which also reduces their value for many forms of testing. When a plant enters decommissioning, the cable owners may be distinct from those who operated the plant and information on the identity and exposure history of any harvestable cables may be difficult to obtain. Pilot studies of in-plant cables by EPRI and cable service providers in partnership with cable program owners represent an opportunity to gather cable condition information that greatly increases the values of the test results.

6.2 Modeling for Cable Performance Prediction

With increases in computing power and computational tools, including artificial intelligence and machine learning, it is anticipated that our ability to correlate difficult-to-measure cables properties from easily measured ones and to predict cable remaining lifetime based on current measurements will also

increase. A few examples of cable material prediction tool development since the EMDA Vol. 5 was published include better analytical simulation of combined thermal and radiation aging and computational prediction of degradation progression. Predictive models are limited by available experimental validation and by the wide range of cable insulation materials and cables constructions in use. Material formulations are largely unknown with any degree of specificity. Formulations are proprietary and many manufacturers of cables used in long term operations are no longer in business. Harvesting and analysis of harvested materials is necessary for calibration and verification of simulation results and absence of harvest material can be another limitation of the potential of modeling and simulation.

Historically, EAB data subjected to combined thermal and radiation aging are visualized by plotting “dose to equivalent damage” (DED) against dose rate on log-log scale and adding temperature values next to each data point [91,94]. The data points were then shifted horizontally to the reference temperature (T_{ref}) using the shift factor (a_T) calculated from Arrhenius temperature dependence with a single activation energy. The procedure is illustrated in Figure 29 and assumes no dose rate effects and the that temperatures fall within the Arrhenius range.

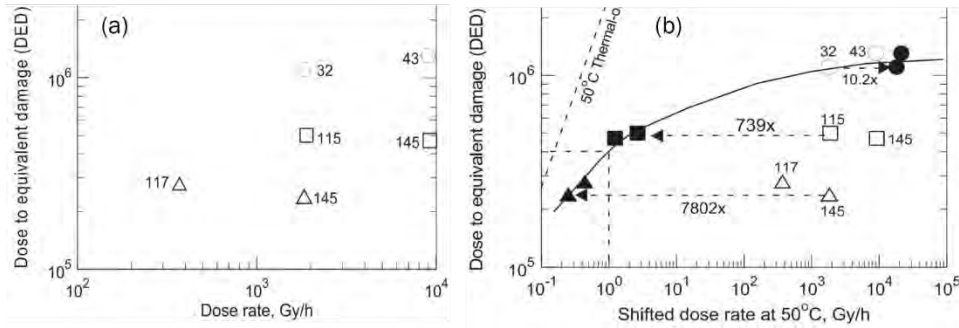


Figure 29. (a) Dose to reach 100% EAB of an EPR material with aging temperature in °C marked beside the data points. (b) Horizontally shifting the data to 50 °C. Filled symbols represent shifted results. [94]

The practice of shifting along the log dose rate axis by the amount of a_T is equivalent to:

$$\log R_1 - \log R_2 = a_T \Rightarrow \log \frac{R_1}{R_2} = \left(\frac{1}{T_1} - \frac{1}{T_2} \right) \times \left(-\frac{E_a}{R} \log e \right),$$

where (R_1 , T_1) and (R_2 , T_2) are the dose rate (R) and temperature (T) before and after shifting. Based on this equation, it is straightforward to plot degradation (in Z axis) with respect to $1/T$ (X axis) and $\log R$ (Y axis), or in a 2D figure with the iso-degradation contours in the $\log R - 1/T$ coordinate (XY plane). The “matched accelerated condition” (MAC) approach proposed in previous work [94] is such a contour plot where each MAC line is an iso-DED contour. The assumptions in MAC approach are the same as in DED or $t-T-R$ superposition. The MAC plot visualizes the *temperature dominant* and *radiation dominant* regions and is a significant improvement over and a potential replacement to the DED approach.

More importantly, improvement in quantitative prediction of aging requires a deeper understanding in degradation kinetics. The BAS mechanism has been used to model the effects of environmental stressors and has successfully explained the anomalous phenomena as outlined in section 5 by a change in the rate-limiting step in different environments. However, the assumptions in BAS may require further examination to include the effects of other processes such as oxygen diffusion and antioxidant depletion. For example, kinetics modeling based on BAS (Figure 9) predicts a plateau on the DED-dose rate plot at the high dose rate end, as shown in Figure 30(a) and in Figure 30(b) with solid lines [91,95]. However, the Fuse model predicts a rapid increase in DED with dose rates at the high dose rate regime, where the transition of slope corresponds to the antioxidant concentration reaching a critical value [95].

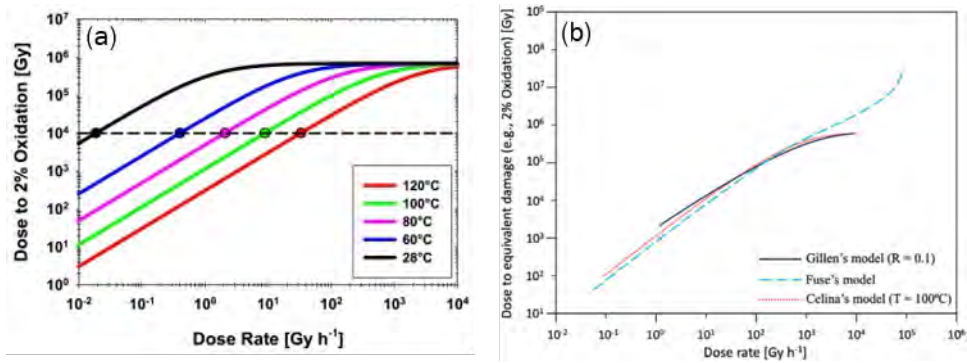


Figure 30. Dose to equivalent damage as a function of dose rate predicted by different models. [95]

Another study regarding quantitative modeling of cable insulation degradation is a “dichotomy model” developed under NEUP Project 15-8258 [96]. The model considers macroscopic degradation as accumulative deactivation of units coined “subcubes” as illustrated in Figure 30. Degraded subcubes cannot contribute to EAB or electrical resistance. Degradation of subcubes follows diffusion or reaction kinetics models. Stretched exponential decay functions were derived for EAB and insulation resistivity and were verified using published experimental data. While the model is at an early stage of development, especially regarding oxidation kinetics, and requires parameterization by curve-fitting EAB data rather than predicting the time-dependent EAB curves (and thus failure time) for given environmental conditions, it does provide a possible pathway to correlate degradation kinetics and mechanical failure. Through Bayesian treatment of a key parameter, the model allows estimation of the uncertainty in EAB curves and predicted lifetime [96,97].

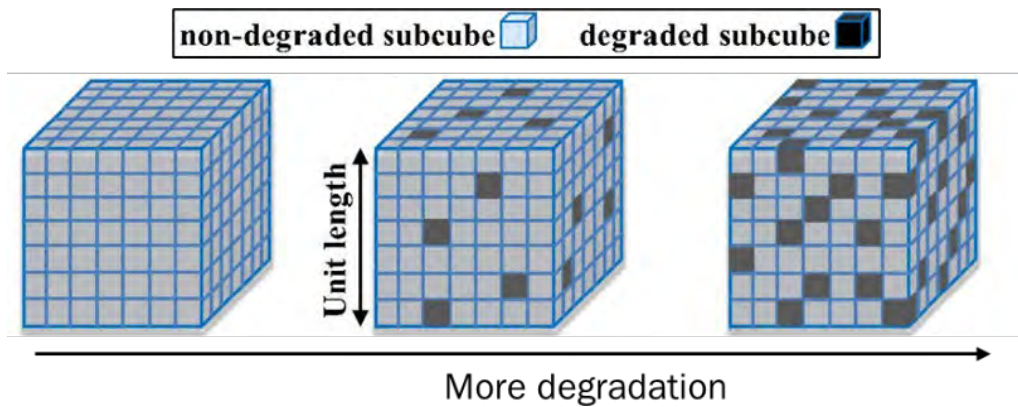


Figure 31. Illustration of dichotomy model [96].

In other work, a micro-mechanical approach has been used by Mohammadi and co-workers to achieve constitutive modeling of the effects of time, ultraviolet radiation, and temperature on elastomers [98]. Such tools and approaches are promising for developing predictive relationships between nuclear cable insulation material composition, exposure, and performance.

6.3 Condition Based Decision Making

The EMDA Vol. 5 identified questions regarding the adequacy of cable longevity assurance based on the historical qualification process, but additional motivations to verify continued cable safe operational status are many. While operating experience has suggested that cable failures are rare, cables in the subsequent license period will have been used far longer than originally anticipated. Cable environments over the long history of the plants might not be precisely known and changes may have occurred over

time in local cable environments. It should be noted that aging of cables, even over the long term, only occurs to a significant degree in cases of adverse local equipment environments (ALEEs) such as in the presence of high temperature process fluid piping, high temperature equipment, or in areas of limited ventilation [99]. Decisions to retain, repair, or replace cables, as well as decision on appropriate re-test intervals, might best be made based on actual measured condition of the cables in question. Condition-based verification or condition-based qualification are potential solutions to ensuring cable reliability independent of knowledge of cable history.

Given the large volume of different types of cables servicing NPPs, prevention and detection of cable failure during the operating lifetime of an NPP is a vital part of cable aging management programs. As such, most NPPs now have cable management programs that implement nondestructive evaluation (NDE) to monitor electrical cable status. While NDE techniques have seen growth and improvement in diagnostic ability and fault detection performance, practical implementation of NDE has a few persisting limitations. First, there is no single NDE method that can comprehensively evaluate cable performance and safety, and therefore a combination of multiple global and local tests is required to collectively provide a high reliability assessment of cable performance. Second, most of the widespread NDE techniques [reflectometry, dielectric spectroscopy (DS), Tan Delta, etc.] require cables to be powered down and/or disconnected on at least one end to implement the test, which contributes to high operation and maintenance costs. Consequently, to improve the efficiency and cost-effectiveness of cable testing, utilities seek improvement in robust NDE techniques for cable assessment. Two burgeoning initiatives aimed at managing time and costs associated with testing are i) online monitoring (i.e., NDE on live or energized cables), and ii) employment of NDE techniques that can be implemented even with components, such as motors, attached. The transition to online monitoring for real-time cable assessment could lower costs associated with the significant down time associated with de-energizing and disconnecting cable systems to perform the testing. Similarly, implementing NDE tests that can be performed while leaving a motor connected could help minimize disconnect and re-connect costs. In the absence of effective online techniques, continued advancement of the diagnostic power and reliability of off-line cable test strategies will support effective and efficient cable aging management.

Numerous examples of research have been conducted to compare known degradation indicators and to find those compatible with online, non-destructive condition monitoring and condition-based qualification (CBQ). Two recent reports are highlighted for their comprehensiveness. One is NISTIR 8391 [63] that was also mentioned in 5.3. The aging conditions of choice are close to service conditions, especially the temperatures being within typical Arrhenius range. Materials are representative of popular insulation and jacket polymers of LV cables. Comments on the results presented in NISTIR 8391 are included in NUREG/CR-7300. The conclusions for each of the “condition monitors” are given below:

- EAB trended best with degradation.
- Compressive modulus from indenter test increased with aging of elastomers (EPR, CSPE, CPE).
- Oxidation induction time or temperature (OIT/OITP) data exhibited large scattering and outliers attributed to artifacts of the test.
- Degradation onset temperature (T_d) at 5% mass loss in a temperature ramp measured by thermogravimetric analysis (TGA) and the temperature at maximum mass loss rate ($\delta w/\delta T$) fluctuated with aging time.
- Increase in carbonyl index from FTIR with aging was observed for jackets but not for insulations. A possible explanation could be that the insulation samples were not separated from the cable assemblies during aging and therefore were not significantly oxidized due to DLO (see 5.1.1). If that is the case, the practice of using degradation of jackets as a precursor of insulation degradation is valid.
- Raman spectroscopy was not effective for cables as inorganic fillers absorbed the incident beam.
- All the methods except EAB were localized and do not necessarily represent the degradation condition of entire cable.

- Frequency domain reflectometry (FDR) test parameters and insulation resistance showed significant scattering and little change with aging.

EPRI 3002026361, “Condition-Based Qualification of Class 1E Cables”, was published in August 2023 [100]. This report included condition monitoring data of XLPO insulation and XLPO jacket, aged at four conditions: (i) 1 kGy/h (0.1 Mrad/h) up to 250 or 311 kGy (25.0 or 31.1 Mrad), followed by 155 °C thermal aging, (ii) thermal-only aging at 165 °C, and (iii) two-stage radiation-only aging with the first stage at 1 kGy/h (0.1 Mrad/h) up to 311 kGy (31.1 Mrad) and the second stage at a dose rate less than 12 kGy/h (1.2 Mrad/h) and total dose up to 600 kGy (60 Mrad). The temperatures and dose rates were high and aimed at depletion of the qualified lifetime (up to 80 years) or up to 90% decrease in EAB. Test methods were chosen referring to International Atomic Energy Agency (IAEA) documents [101–103]. Results were consistent with the findings in NISTIR 8391. Specifically,

- EAB provided the best evaluation of cable condition especially near end of life.
- Indenter modulus showed large deviation as expected for XLPO.
- OIT/OITP trended well with aging for condition (i) but not for condition (ii) or (iii).
- Neither Td at 5% mass loss nor temperature at maximum mass loss showed significant change with aging.
- Carbonyl index did not change with aging. It was noted that the carbonyl index of the new sample was around 1, larger than the typical range (0 to 0.5) where carbonyl index increases with aging.
- Time domain reflectometry (TDR) and FDR were useful to find fault locations such as open circuits and short circuits but were insensitive to localized insulation aging or other minor changes.

Since mechanical durability and dielectric insulation properties are the material properties of consequence to the safety functions of cable insulations, the importance of EAB might not be replaced by any other chemical or mechanical properties. Practical cable aging management based on condition monitoring data relies on acceptance criteria with easily interpreted test outcomes, such as corresponding to ‘reliable’, ‘test again soon’, or ‘not reliable’ cable status. For each cable testing method, therefore, sufficient understanding of the correlation between the test results and the material state is required. In the absence of established acceptance criteria, many test methods trend well with aging, but are less useful for single snapshot measurements. New test methods often must be developed with consensus-based standard usage (e.g., IEEE) prior to endorsed usage.

7. Summary

This report summarized research relevant to cable aging knowledge gaps identified in NUREG/CR-7153, “Expanded Materials Degradation Assessment (EMDA), Volume 5: Aging of Cables and Cable Systems” [5], performed since the EMDA was published in 2014. It began with a discussion of the status of long-term operation of U.S. nuclear power plants and the most common cables found in NPP containment. Next, the major polymer cable insulations, and the mechanisms of concern for degradation of those polymers in service were reviewed. A description of the environmental qualification process historically used for safety-related cables was provided as was a review of the potential concerns with that process highlighted in the EMDA Vol. 5. Research addressing each of these was then reviewed. Finally, three components of a strategy to support continued safe operation of aging cables were proposed: condition-based verification, informed by targeted material aging studies and advanced modeling.

For cable insulation, the most important property is dielectric strength. Mechanical durability is also important if the cable is subject to handling, cyclic vibration, or extreme compression/tension. Mechanisms of deterioration of dielectric and mechanical properties were presented in Section 3, which vary between XLPE and EPR-based insulations arising from differences in their molecular structure and

product formulation. Reviewing the degradation mechanisms in thermal and radiation aging provides a unified and systematic knowledge base to explain anomalous phenomena identified as knowledge gaps (Section 5). Specifically,

- Embrittlement of XLPE and semi-crystalline polymers involves recrystallization of broken chains favored by free radical propagation and branching steps where oxygen is a reactant. It explains the inverse temperature effects and subsequent thermal annealing observed for XLPE, and the observation that thermal-only aging followed by radiation-only aging is the most degradative scenario for XLPE and EPR with high degree of crystallinity. (5.3)
- For elastomeric EPR, the slow decomposition of metastable hydroperoxides, the intermediate degradation products, can explain the observed synergistic effect that radiation-only aging followed by thermal-only aging is the most severe condition. (5.3)
- Higher dose rates lead to higher initiation rates but not necessarily higher overall degradation rates. The extra free radicals generated at high dose rates may not propagate to cause chain scission and embrittlement, which may be the reason for dose rate effects observed for XLPE. (5.2.1)
- The oxygen-involved propagation (causing chain scission) is more competitive over termination (favoring crosslinking) at lower temperatures, leading to deviation from Arrhenius temperature dependence. (5.1.2)
- At high temperatures, reaction rates are significantly accelerated so that the diffusion of oxygen becomes rate-limiting. Spatially inhomogeneous aging or diffusion limited oxygen along sample thickness can be visualized with various techniques. (5.1.1)

The moisture effects and affected dielectric properties represent a relatively distinct area of interest from the thermal-radiation aging. EPRI guidelines on Tan Delta testing and acceptance criteria [83–86] were statistically examined [87] and confirmed as an reasonable primary tool for condition monitoring of MV cables in wet or submerged environments. (5.4)

Environmental service condition data collected by EPRI concluded that the actual temperatures and integrated total dose are lower than design values [40 ~ 50 °C, 50 Mrad (500 kGy)]. (5.5)

Knowledge gaps identified in the EMDA Vol. 5 represent concerns that the assumptions made in 40-year environmental qualification of cables may be weak, that the pre-aging of cables prior to LOCA testing may have represented less than 40-year equivalence, and that consequently the EQ process may not be conservative and thereby overpredict cable useful lifetime. While cable failures were relatively few in the first 40-60 years of plant operation, the concern is that lack of conservatism in the 40-year qualification is a more serious issue in licensing up to 80 years. Subsequent research by DOE and others in the years following publication of the EMDA Vol. 5, as reviewed herein, found that the Arrhenius and equal dose/equal damage assumptions of thermal and radiation aging behavior on which the historical qualification process was based hold for some relevant cable materials, accelerated aging conditions, and performance metrics and do not hold for others. While the pre-aging process appears to be not conservative in some cases, it appeared to be conservative in others.

Three approaches to increase confidence in the continued reliable performance of existing nuclear electrical cables are: 1) advance comprehensive cable condition monitoring programs using existing and newly developed tools to inform decisions to repair, replace, or retain aged cables, 2) pursue additional aging studies and the characterization of harvested materials for greater understanding of nuclear cable insulation degradation in the nuclear plant environment, and 3) utilize modeling and simulation to predict cable performance from material measures. Use of a testing-based approach is anticipated to be the most promising strategy for future cable aging management in light water reactors—supported by targeted material aging studies, modeling and simulation of material composition/exposure/performance relationships, and evaluation of harvested cables.

8. References

- [1] NRC, *Backgrounder on Reactor License Renewal*, U.S. Nuclear Regulatory Commission. Last Reviewed/Updated Monday, January 03, 2022. <https://www.nrc.gov/reading-rm/doc-collections/fact-sheets/fs-reactor-license-renewal.html>. Accessed September 15, 2023.
- [2] NRC, *Operating U.S. Nuclear Research and Test Reactors – Regulated by the NRC*, Dataset last updated February 23, 2023. U.S. Nuclear Regulatory Commission. <http://www.nrc.gov/reading-rm/doc-collections/datasets/reactors-operating.xlsx>. Accessed September 15, 2023.
- [3] NRC, *Generic Aging Lessons Learned for Subsequent License Renewal (GALL-SLR) Report*, NUREG-2191, U.S. Nuclear Regulatory Commission, 2017. <https://www.nrc.gov/reading-rm/doc-collections/nuregs/staff/sr2191/r0/index.html>.
- [4] NRC, *Generic Aging Lessons Learned (GALL) Report – Final Report*, NUREG-1801, Revision 2, U.S. Nuclear Regulatory Commission, 2010. <https://www.nrc.gov/reading-rm/doc-collections/nuregs/staff/sr1801/r2/index.html>.
- [5] NRC, *Expanded Materials Degradation Assessment (EMDA): Aging of Cables and Cable Systems*, NUREG/CR-7153, Vol. 5 (ORNL/TM-2013/532), U.S. Nuclear Regulatory Commission, 2014. <https://www.nrc.gov/docs/ML1427/ML14279A461.pdf>.
- [6] DOE, *Light Water Reactor Sustainability (LWRS) Program*, U.S. Department of Energy. <https://lwrs.inl.gov>. Accessed September 15, 2023.
- [7] IEEE, *IEEE Standard for Design and Installation of Cable Systems for Class 1E Circuits in Nuclear Power Generating Stations*, IEEE Std 690-2018 (Revision IEEE Std 690-2004), Institute of Electrical and Electronics Engineers, 2019. <https://doi.org/10.1109/IEEESTD.2019.8694187>.
- [8] IEEE, *IEEE Standards Dictionary*, “Medium-Voltage Power Cables,” Institute of Electrical and Electronics Engineers. <https://ieeexplore.ieee.org/browse/standards/dictionary?activeStatus=true&queryText=medium%20voltage%20power%20cable>. Accessed September 15, 2023.
- [9] ICEA, *Concentric Neutral Cables Rated 5 Through 46KV*, ANSI/ICEA S-94-649, Insulated Cable Engineers Association, Inc., 2021. <https://www.icea.net/docs>.
- [10] EPRI, *Plant Engineering: Cable Polymer Handbook - Medium Voltage Insulations*, EPRI 3002005322, Electric Power Research Institute, 2015. <https://www.epri.com/research/products/000000003002005322>.
- [11] SNL, *Aging Management Guideline for Commercial Nuclear Power Plants - Electrical Cable and Terminations*, SAND96-0344, Sandia National Laboratories, 1996. <https://www.nrc.gov/docs/ML0311/ML031140264.pdf>.
- [12] EPRI, *Low-Voltage Environmentally-Qualified Cable License Renewal Industry Report – Rev. 1*, EPRI TR-103841, Electric Power Research Institute, 1994. <https://www.epri.com/research/products/TR-103841>.
- [13] NEI, *Medium Voltage Underground Cable White Paper*, NEI 06-05, Nuclear Energy Institute, April 2006. <https://www.nrc.gov/docs/ML0612/ML061220137.pdf>
- [14] SNL, *Submerged Medium Voltage Cable Systems at Nuclear Power Plants: A Review of Research Efforts Relevant to Aging Mechanisms and Condition Monitoring*, SAND-2015-1794, Sandia National Laboratories, 2015. <https://doi.org/10.2172/1177756>.
- [15] V. Vahedy, “Polymer Insulated High Voltage Cables,” *IEEE Electr. Insul. Mag.* **22**, 13–18 (2006). <https://doi.org/10.1109/MEI.2006.1639025>.
- [16] EPRI, *Cable Polymer Material Handbook—Low Voltage Power and Control Cable*, EPRI 3002010637, Electric Power Research Institute, 2017.

- <https://www.epri.com/research/products/3002010637>.
- [17] C.L. Wysocki, *Reinforcement of Ethylene Propylene Rubber (EPR) and Ethylene Propylene Diene Rubber (EPDM) by Zinc Dimethacrylate*, University of Akron, 2006. http://rave.ohiolink.edu/etdc/view?acc_num=akron1145038716.
- [18] R.J. Arhart, "The Chemistry of Ethylene Propylene Insulation. II," *IEEE Electr. Insul. Mag.* **9** 11–14 (1993). <https://doi.org/10.1109/57.245979>.
- [19] S.-Q. Liu, W.-G. Gong, B.-C. Zheng, "The Effect of Peroxide Cross-Linking on the Properties of Low-Density Polyethylene," *J. Macromol. Sci. Part B.* **53** 67–77 (2014). <https://doi.org/10.1080/00222348.2013.789360>.
- [20] X. Zhang, H. Yang, Y. Song, Q. Zheng, "Influence of Crosslinking on Crystallization, Rheological, and Mechanical Behaviors of High Density Polyethylene/Ethylene-Vinyl Acetate Copolymer Blends," *Polym. Eng. Sci.* **54** 2848–2858 (2014). <https://doi.org/10.1002/pen.23843>.
- [21] D. Gheysari, A. Behjat, M. Haji-Saeid, "The Effect of High-Energy Electron Beam on Mechanical and Thermal Properties of LDPE and HDPE," *Eur. Polym. J.* **37** 295–302 (2001). [https://doi.org/10.1016/S0014-3057\(00\)00122-1](https://doi.org/10.1016/S0014-3057(00)00122-1).
- [22] S. Nilsson, T. Hjertberg, A. Smedberg, B. Sonerud, "Influence of Morphology Effects on Electrical Properties in XLPE," *J. Appl. Polym. Sci.* **121** 3483–3494 (2011). <https://doi.org/10.1002/app.34006>.
- [23] H. Ahmad, D. Rodrigue, "Crosslinked Polyethylene: a Review on the Crosslinking Techniques, Manufacturing Methods, Applications, and Recycling," *Polym. Eng. Sci.* **62** 2376–2401 (2022). <https://doi.org/10.1002/pen.26049>.
- [24] M. Celina, G.A. George, "Characterisation and Degradation Studies of Peroxide and Silane Crosslinked Polyethylene," *Polym. Degrad. Stab.* **48** 297–312 (1995). [https://doi.org/10.1016/0141-3910\(95\)00053-O](https://doi.org/10.1016/0141-3910(95)00053-O).
- [25] L.M. Smith, H.M. Aitken, M.L. Coote, "The Fate of the Peroxyl Radical in Autoxidation: How Does Polymer Degradation Really Occur?," *Acc. Chem. Res.* **51** 2006–2013 (2018). <https://doi.org/10.1021/acs.accounts.8b00250>.
- [26] J.L. Bolland, G. Gee, "Kinetic Studies in The Chemistry of Rubber and Related Materials. II. The Kinetics of Oxidation of Unconjugated Olefins," *Trans. Faraday Soc.* **42** 236 (1946). <https://doi.org/10.1039/TF9464200236>.
- [27] J.L. Bolland, G. Gee, "Kinetic Studies in The Chemistry of Rubber and Related Materials. III. Thermochemistry and Mechanisms of Olefin Oxidation," *Trans. Faraday Soc.* **42** 244–252 (1946). <https://doi.org/10.1039/TF9464200244>.
- [28] L. Bateman, G. Gee, E.K. Rideal, "A Kinetic Investigation of the Photochemical Oxidation of Certain Non-Conjugated Olefins," *Proc. R. Soc. London. Ser. A. Math. Phys. Sci.* **195** 376–391 (1948). <https://doi.org/10.1098/rspa.1948.0125>.
- [29] G. Geuskens, M.S. Kabamba, "Photo-oxidation of Polymers—Part V: A New Chain Scission Mechanism in Polyolefins," *Polym. Degrad. Stab.* **4** 69–76 (1982). [https://doi.org/10.1016/0141-3910\(82\)90007-6](https://doi.org/10.1016/0141-3910(82)90007-6).
- [30] B. Fayolle, E. Richaud, X. Colin, J. Verdu, "Review: degradation-induced embrittlement in semi-crystalline polymers having their amorphous phase in rubbery state," *J. Mater. Sci.* **43** 6999–7012 (2008). <https://doi.org/10.1007/s10853-008-3005-3>.
- [31] B. Fayolle, X. Colin, L. Audouin, J. Verdu, "Mechanism of Degradation Induced Embrittlement in Polyethylene," *Polym. Degrad. Stab.* **92** 231–238 (2007). <https://doi.org/10.1016/j.polymdegradstab.2006.11.012>.
- [32] C. Blivet, J.-F. Larché, Y. Israël, P.-O. Bussière, J.-L. Gardette, "Thermal Oxidation of Cross-linked PE and EPR Used as Insulation Materials: Multi-scale Correlation Over a Wide Range of

- Temperatures,” *Polym. Test.* **93** 106913 (2021).
<https://doi.org/10.1016/j.polymertesting.2020.106913>.
- [33] S. Zha, H. Lan, N. Lin, T. Meng, “Degradation and Characterization Methods for Polyethylene Gas Pipes after Natural and Accelerated Aging,” *Polym. Degrad. Stab.* **208** 110247 (2023).
<https://doi.org/10.1016/j.polymdegradstab.2022.110247>.
- [34] T. Salivon, R. Comte, X. Colin, “Thermal Aging of Electrical Cable Insulation Made of Cross-Linked Low Density Polyethylene for Under-Hood Application in Automotive Industry,” *J. Vinyl Addit. Technol.* **28** 418–429 (2022). <https://doi.org/10.1002/vnl.21916>.
- [35] IEEE, *IEEE Guide for Field Testing and Evaluation of the Insulation of Shielded Power Cable Systems Rated 5 kV and Above*, IEEE Std 400-2012 (Revision of IEEE Std 400-2001), Institute of Electrical and Electronics Engineers, 2012. <https://doi.org/10.1109/IEEESTD.2012.6213052>.
- [36] NEETRAC, *Diagnostic Testing of Underground Cable Systems (Cable Diagnostic Focused Initiative)*, DOE Award No. DE-FC02-04CH11237 (NEETRAC Project Numbers: 04-211/04-212/09-166), National Electric Energy Testing, Research & Applications Center, Georgia Tech Research Corporation, 2010. <https://doi.org/10.2172/1004068>.
- [37] S. Boggs, J. Xu, “Water Treeing - Filled Versus Unfilled Cable Insulation,” *IEEE Electr. Insul. Mag.* **17** 23–29 (2001). <https://doi.org/10.1109/57.901616>.
- [38] J. Jung, “Water Trees in Cables: Generation and Detection,” *IEE Proc. - Sci. Meas. Technol.* **146** 253-259 (1999). <https://doi.org/10.1049/ip-smt:19990486>.
- [39] IEEE, *IEEE Standard for Type Test of Class Ie Electric Cables, Field Splices, and Connections for Nuclear Power Generating Stations*, ANSI/IEEE Std 383-1974, Institute for Electrical and Electronics Engineers, 1974. <https://doi.org/10.1109/IEEESTD.1974.120627>.
- [40] IEEE, *IEEE Standard for Qualifying Class Ie Electric Cables and Field Splices for Nuclear Power Generating Stations*, IEEE Std 383-2003 (Revision of IEEE Std 383-1974), Institute for Electrical and Electronics Engineers, 2004. <https://doi.org/10.1109/IEEESTD.2004.94567>.
- [41] IEEE, *IEEE Standard for Qualifying Electric Cables and Splices for Nuclear Facilities*, IEEE Std 383-2015 (Revision of IEEE Std 383-2003), Institute for Electrical and Electronics Engineers, 2015. <https://doi.org/10.1109/IEEESTD.2015.7287711>.
- [42] IEEE, *IEEE Trial-Use Standard: General Guide for Qualifying Class I Electric Equipment for Nuclear Power Generating Stations*, IEEE No 323-1971, Institute for Electrical and Electronics Engineers, 1971. <https://doi.org/10.1109/IEEESTD.1971.6529090>.
- [43] IEEE, *IEEE Standard for Qualifying Class Ie Equipment for Nuclear Power Generating Stations*, IEEE Std 323-1974 (Revision of IEEE 323-1971 ANSI N41.5-1971), Institute for Electrical and Electronics Engineers, 1974. <https://doi.org/10.1109/IEEESTD.1974.6568022>.
- [44] IEEE, *IEEE Standard for Qualifying Class Ie Equipment for Nuclear Power Generating Stations*, IEEE Std 323-1983, Institute for Electrical and Electronics Engineers, 1983.
<https://doi.org/10.1109/IEEESTD.1983.82408>.
- [45] IEEE, *IEEE Standard for Qualifying Class Ie Equipment for Nuclear Power Generating Stations*, IEEE Std 323-2003 (Revision IEEE Std 323-1983), Institute for Electrical and Electronics Engineers, 2004. <https://doi.org/10.1109/IEEESTD.2004.94415>.
- [46] IEC/IEEE, *IEC/IEEE International Standard - Nuclear facilities -- Electrical equipment important to safety -- Qualification*, IEC/IEEE 60780-323 Ed. 1.0 2016-02, International Electrotechnical Commission / Institute for Electrical and Electronics Engineers, 2016.
<https://doi.org/10.1109/IEEESTD.2016.7425113>.
- [47] ASTM, *Standard Guide for Statistical Analysis of Accelerated Service Life Data*, ASTM G172-19, 2019. <https://doi.org/10.1520/G0172-19>.
- [48] IEEE, *IEEE Recommended Practice - General Principles for Temperature Limits in the Rating of*

- Electrical Equipment and for the Evaluation of Electrical Insulation*, IEEE Std 1-2000, Institute of Electrical and Electronics Engineers, 2001. <https://doi.org/10.1109/IEEESTD.2001.92768>.
- [49] IEEE, *IEEE Standard for the Preparation of Test Procedures for the Thermal Evaluation of Solid Electrical Insulating Materials*, IEEE Std 98-2016 (Revision IEEE Std 98-2002), Institute of Electrical and Electronics Engineers, 2016. <https://doi.org/10.1109/IEEESTD.2016.7469275>.
- [50] IEEE, *IEEE Recommended Practice for the Preparation of Test Procedures for the Thermal Evaluation of Insulation Systems for Electrical Equipment*, IEEE Std 99-2019 (Revision IEEE Std 99-2007), Institute of Electrical and Electronics Engineers, 2020. <https://doi.org/10.1109/IEEESTD.2020.9179115>.
- [51] ANSI/IEEE, *IEEE Guide for the Statistical Analysis of Thermal Life Test Data*, ANSI/IEEE Std 101-1987(R2010) (Revision of IEEE Std 101-1972), American National Standards Institute / Institute of Electrical and Electronics Engineers, 1988. <https://ieeexplore.ieee.org/document/7473795>.
- [52] M. Celina, J. Wise, D.K. Ottesen, K.T. Gillen, R.L. Clough, “Oxidation Profiles of Thermally Aged Nitrile Rubber,” *Polym. Degrad. Stab.* **60** 493–504 (1998). [https://doi.org/10.1016/S0141-3910\(97\)00113-4](https://doi.org/10.1016/S0141-3910(97)00113-4).
- [53] M. Celina, J. Wise, D.K. Ottesen, K.T. Gillen, R.L. Clough, “Correlation of Chemical and Mechanical Property Changes During Oxidative Degradation of Neoprene,” *Polym. Degrad. Stab.* **68** 171–184 (2000). [https://doi.org/10.1016/S0141-3910\(99\)00183-4](https://doi.org/10.1016/S0141-3910(99)00183-4).
- [54] M. Spencer, W. Fuchs, Y. Ni, D. Li, M.R. Pallaka, A. Arteaga, L.S. Fifield, “Color as a Tool for Quantitative Analysis of Heterogeneous Polymer Degradation,” *Mater. Today Chem.* **29** 101417 (2023). <https://doi.org/https://doi.org/10.1016/j.mtchem.2023.101417>.
- [55] J. Wise, K.T. Gillen, R.L. Clough, “Quantitative Model for the Time Development of Diffusion-limited Oxidation Profiles,” *Polymer.* **38** 1929–1944 (1997). [https://doi.org/10.1016/S0032-3861\(96\)00716-1](https://doi.org/10.1016/S0032-3861(96)00716-1).
- [56] K.T. Gillen, R.L. Clough, C.A. Quintana, “Modulus Profiling of Polymers,” *Polym. Degrad. Stab.* **17** 31–47 (1987). [https://doi.org/10.1016/0141-3910\(87\)90046-2](https://doi.org/10.1016/0141-3910(87)90046-2).
- [57] PNNL, *Inhomogeneous Aging of Nuclear Power Plant Electrical Cable Insulation*, PNNL-31443, Pacific Northwest National Laboratory, 2021. https://lwrsl.inl.gov/MaterialsAgingandDegradation/InhomogeneousAgingNPP_ElectricalCableInsulation.pdf.
- [58] M.C. Celina, “Review of Polymer Oxidation and its Relationship with Materials Performance and Lifetime Prediction,” *Polym. Degrad. Stab.* **98** 2419–2429 (2013). <https://doi.org/10.1016/j.polymdegradstab.2013.06.024>.
- [59] M. Celina, K.T. Gillen, R.A. Assink, “Accelerated Aging and Lifetime Prediction: Review of Non-Arrhenius Behaviour Due to Two Competing Processes,” *Polym. Degrad. Stab.* **90** 395–404 (2005). <https://doi.org/10.1016/j.polymdegradstab.2005.05.004>.
- [60] C. Blivet, J.-F. Larché, Y. Israël, P.-O. Bussière, “Non-Arrhenius Behavior: Influence of the Crystallinity on Lifetime Predictions of Polymer Materials Used in the Cable and Wire Industries,” *Polym. Degrad. Stab.* **199** 109890 (2022). <https://doi.org/10.1016/j.polymdegradstab.2022.109890>.
- [61] K.T. Gillen, R. Bernstein, D.K. Derzon, “Evidence of Non-Arrhenius Behaviour From Laboratory Aging and 24-year Field Aging of Polychloroprene Rubber Materials,” *Polym. Degrad. Stab.* **87** 57–67 (2005). <https://doi.org/10.1016/j.polymdegradstab.2004.06.010>.
- [62] J. Wise, K.T. Gillen, R.L. Clough, “An Ultrasensitive Technique for Testing The Arrhenius Extrapolation Assumption for Thermally Aged Elastomers,” *Polym. Degrad. Stab.* **49** 403–418 (1995). [https://doi.org/10.1016/0141-3910\(95\)00137-B](https://doi.org/10.1016/0141-3910(95)00137-B).
- [63] NIST, *Assessment of Condition Monitoring Methods of Electrical Cables*, NISTIR 8391, 2021.

- <https://adamswebsearch2.nrc.gov/webSearch2/main.jsp?AccessionNumber=ML22298A160>.
- [64] ASTM, *Standard Test Methods for Kinetic Parameters by Differential Scanning Calorimetry Using Isothermal Methods*, ASTM E2070-13, 2018. <https://doi.org/10.1520/E2070-13R18>.
- [65] ASTM, *Standard Practice for Statistical Treatment of Thermoanalytical Data*, ASTM E1970-23, 2023. <https://doi.org/10.1520/E1970-23>.
- [66] A.B. Reynolds, R.M. Bell, N.M.N. Bryson, T.E. Doyle, M.B. Hall, L.R. Mason, L. Quintric, P.L. Terwilliger, “Dose-rate Effects on the Radiation-induced Oxidation of Electric Cable Used in Nuclear Power Plants,” *Radiat. Phys. Chem.* **45** 103–110 (1995). [https://doi.org/10.1016/0969-806X\(94\)E0003-2](https://doi.org/10.1016/0969-806X(94)E0003-2).
- [67] I. Kuriyama, N. Hayakawa, Y. Nakase, J. Ogura, H. Yagyu, K. Kasai, “Effect of Dose Rate on Degradation Behavior of Insulating Polymer Materials,” *IEEE Trans. Electr. Insul.* **EI-14** 272–277 (1979). <https://doi.org/10.1109/TEI.1979.298231>.
- [68] PNNL, *Dose Rate Effects on Degradation of Nuclear Power Plant Electrical Cable Insulation at a Common Dose*, PNNL-34068, Pacific Northwest National Laboratories, 2023. https://www.pnnl.gov/main/publications/external/technical_reports/PNNL-34068.pdf.
- [69] K.T. Gillen, R.L. Clough, N.J. Dhooge, “Density Profiling of Polymers,” *Polymer.* **27** 225–232 (1986). [https://doi.org/10.1016/0032-3861\(86\)90330-7](https://doi.org/10.1016/0032-3861(86)90330-7).
- [70] A. Tidjani, Y. Watanabe, “Gamma-oxidation of Linear Low-density Polyethylene: The Dose–rate Effect of Irradiation on Chemical and Physical Modifications,” *J. Polym. Sci. Part A Polym. Chem.* **33** 1455–1460 (1995). <https://doi.org/https://doi.org/10.1002/pola.1995.080330906>.
- [71] K.T. Gillen, R.L. Clough, “Time-temperature-dose Rate Superposition: A Methodology for Extrapolating Accelerated Radiation Aging Data to Low Dose Rate Conditions,” *Polym. Degrad. Stab.* **24** 137–168 (1989). [https://doi.org/10.1016/0141-3910\(89\)90108-0](https://doi.org/10.1016/0141-3910(89)90108-0).
- [72] M. Ferrari, S. Pandini, A. Zenoni, G. Donzella, D. Battini, A. Avanzini, A. Salvini, F. Zelaschi, A. Andrighetto, F. Bignotti, “Degradation of EPDM and FPM Elastomers Irradiated at Very High Dose Rates in Mixed Gamma and Neutron Fields,” *Polym. Eng. Sci.* **59** 2522–2532 (2019). <https://doi.org/10.1002/pen.25249>.
- [73] J. Wise, K.T. Gillen, R.L. Clough, “Time Development of Diffusion-Limited Oxidation Profiles in a Radiation Environment,” *Radiat. Phys. Chem.* **49** 565–573 (1997). [https://doi.org/10.1016/S0969-806X\(96\)00185-5](https://doi.org/10.1016/S0969-806X(96)00185-5).
- [74] SNL, *The Effect of Thermal and Irradiation Aging Simulation Procedures on Polymer Properties*, NUREG/CR-3629 (SAND83-2651), Sandia National Laboratories, 1984. <https://www.nrc.gov/docs/ML0622/ML062260295.pdf>.
- [75] SNL, *The Effect of LOCA Simulation Procedures on Ethylene Propylene Rubber’s Mechanical and Electrical Properties*, NUREG/CR-3538 (SAND83-1258), Sandia National Laboratories, 1983. <https://www.nrc.gov/docs/ML1335/ML13357A667.pdf>.
- [76] PNNL, *Sequential Versus Simultaneous Aging of XLPE and EPDM Nuclear Cable Insulation Subjected to Elevated Temperature and Gamma Radiation (Final Results)*, PNNL-30041 Rev. 1, Pacific Northwest National Laboratory, 2020. https://lwrs.inl.gov/Materials%20Aging%20and%20Degradation/Seq_vs_Sim_Aging_XLPE_EPDM_Nuclear_Cable.pdf
- [77] R.L. Clough, K.T. Gillen, “Combined Environment Aging Effects: Radiation-thermal Degradation of Polyvinylchloride and Polyethylene,” *J. Polym. Sci. Polym. Chem. Ed.* **19** 2041–2051 (1981). <https://doi.org/10.1002/pol.1981.170190816>.
- [78] G. Geuskens, F. Debie, M.S. Kabamba, G. Nedelkos, “New Aspects of the Photooxidation of Polyolefins,” *Polym. Photochem.* **5** 313–331 (1984). [https://doi.org/10.1016/0144-2880\(84\)90040-X](https://doi.org/10.1016/0144-2880(84)90040-X).

- [79] M. Celina, K.T. Gillen, J. Wise, R.L. Clough, “Anomalous Aging Phenomena in a Crosslinked Polyolefin Cable Insulation,” *Radiat. Phys. Chem.* **48** 613–626 (1996). [https://doi.org/10.1016/0969-806X\(96\)00083-7](https://doi.org/10.1016/0969-806X(96)00083-7).
- [80] M. Celina, K.T. Gillen, R.L. Clough, “Inverse Temperature and Annealing Phenomena During Degradation of Crosslinked Polyolefins,” *Polym. Degrad. Stab.* **61** 231–244 (1998). [https://doi.org/10.1016/S0141-3910\(97\)00142-0](https://doi.org/10.1016/S0141-3910(97)00142-0).
- [81] PNNL, *Inverse Temperature Effects in Nuclear Power Plant Electrical Cable Insulation*, PNNL-33296, Pacific Northwest National Laboratory, 2022. <https://lwrns.inl.gov/Materials%20Aging%20and%20Degradation/InverseTemperatureEffectsInNP.P.pdf>.
- [82] UMD/ORNL, *Quantifying Properties for a Mechanistic, Predictive Understanding of Aqueous Impact on Aging of Medium and Low Voltage AC and DC Cabling in Nuclear Power Plants*, DOE-UMDORNL-NE0008540, University of Minnesota-Duluth / Oak Ridge National Laboratory, 2021. <https://www.osti.gov/biblio/1774077>.
- [83] EPRI, *Medium Voltage Cable Aging Management Guide, Revision 1*, EPRI 1021070, Electric Power Research Institute, 2010. <https://www.epri.com/research/products/00000000001021070>.
- [84] EPRI, *Plant Engineering: Evaluation and Insights from Nuclear Power Plant Tan Delta Testing and Data Analysis*, EPRI 1025262, Electric Power Research Institute, 2012. <https://www.epri.com/research/products/00000000001025262>.
- [85] EPRI, *Plant Engineering, Aging Management Program Guidance for Medium-Voltage Cable Systems for Nuclear Power Plants, Revision 1*, EPRI 3002000557, Electric Power Research Institute, 2013. <https://www.epri.com/research/products/000000003002000557>.
- [86] EPRI, *Plant Engineering: Evaluation and Insights from Nuclear Power Plant Tan Delta Testing and Data Analysis - Update*, EPRI 3002005321, Electric Power Research Institute, 2015. <https://www.epri.com/research/products/000000003002005321>.
- [87] PNNL, *Assessment of EPRI’s Tan Delta Approach to Manage Cables in Submerged Environments: Statistical Review of EPRI Data*, PNNL-28542-1, Pacific Northwest National Laboratory, 2020. <https://doi.org/10.2172/1713064>.
- [88] EPRI, *Long-Term Operations: Normal Temperature and Radiation Dose to Installed Cable for U.S. Nuclear Power Plants in Containment*, EPRI 3002000816, Electric Power Research Institute, 2013. <https://www.epri.com/research/products/000000003002000816>.
- [89] EPRI, *Results of Radiation and Temperature Monitors Research for Installed Cables at U.S. Nuclear Power Plants in Support of Long-Term Operations*, EPRI 3002010404, Electric Power Research Institute, 2017. <https://www.epri.com/research/products/000000003002010404>.
- [90] SNL, *Nuclear Energy Plant Optimization (NEPO) Final Report on Aging and Condition Monitoring of Low-Voltage Cable Materials*, SAND2005-7331, Sandia National Laboratories, 2005. <https://doi.org/10.2172/875986>.
- [91] M. Celina, E. Linde, D. Brunson, A. Quintana, N. Giron, “Overview of Accelerated Aging and Polymer Degradation Kinetics for Combined Radiation-Thermal Environments,” *Polym. Degrad. Stab.* **166** 353–378 (2019). <https://doi.org/10.1016/j.polymdegradstab.2019.06.007>.
- [92] SNL, *Nuclear Power Plant Cable Materials-Review of Qualification and Currently Available Aging Data for Margin Assessments in Cable Performance*, SAND2013-2388, Sandia National Laboratories, 2013. <https://doi.org/10.2172/1096518>.
- [93] PNNL, *Evaluation of Oxygen Consumption as a Sensitive Measure of Electrical Cable Polymer Insulation Degradation*, PNNL-31954, Pacific Northwest National Laboratory, 2021. <https://www.osti.gov/biblio/2280700>.
- [94] K.T. Gillen, M. Celina, “Predicting Polymer Degradation and Mechanical Property Changes for

- Combined Radiation-Thermal Aging Environments,” *Rubber Chem. Technol.* **91** 27–63 (2018). <https://doi.org/10.5254/rct.18.81679>.
- [95] T. Chen, T.-Y. Chang, B.A. Konstanczer, M.A. Mostaan, C.J. Palmer, “Review of Qualification and Modeling for Radiation-induced Polymer Degradation,” *Front. Nucl. Eng.* **2** (2023). <https://www.frontiersin.org/articles/10.3389/fnuen.2023.1287370>.
- [96] A. Mosleh, M. Al-Sheikhly, Y.-S. Chang, R. Reister, *Physics-Based Probabilistic Model of the Effects of Ionizing Radiation on Polymeric Insulators of Electric Cables used in Nuclear Power Plants*, Project No. 15-8258, University of California-Los Angeles / University of Maryland, 2019. <https://doi.org/10.2172/1497835>.
- [97] Y.-S. Chang, A. Mosleh, “Probabilistic Model of Degradation of Cable Insulations In Nuclear Power Plants,” *Proc. Inst. Mech. Eng. Part O J. Risk Reliab.* **233** 803–814 (2019). <https://doi.org/10.1177/1748006X19827127>.
- [98] H. Mohammadi, V. Morovati, A.-E. Korayem, E. Poshtan, R. Dargazany, “Constitutive Modeling of Elastomers During Photo- and Thermo-oxidative Aging,” *Polym. Degrad. Stab.* **191** 109663 (2021). <https://doi.org/10.1016/j.polymdegradstab.2021.109663>.
- [99] EPRI, *Guideline for the Management of Adverse Localized Equipment*, EPRI TR-109619, Electric Power Research Institute, 1999. <https://www.epri.com/research/products/TR-109619>.
- [100] EPRI, *Condition-Based Qualification of Class 1E Cables*, EPRI 3002026361, Electric Power Research Institute, 2023. <https://www.epri.com/research/products/000000003002026361>.
- [101] IAEA, *Benchmark Analysis for Condition Monitoring Test Techniques of Aged Low Voltage Cables in Nuclear Power Plants Final Results of a Coordinated Research Project*, IAEA-TECDOC-1825, International Atomic Energy Agency, 2017. <http://www-pub.iaea.org/MTCD/Publications/PDF/TE-1825web.pdf>.
- [102] IAEA, *Assessment and Management of Ageing of Major Nuclear Power Plant Components Important to Safety: In-containment Instrumentation and Control Cables. Vol. II*, IAEA-TECDOC-1188 (V.2), International Atomic Energy Agency, 2000. https://inis.iaea.org/collection/NCLCollectionStore/_Public/31/065/31065258.pdf?r=1.
- [103] IAEA, *Assessing and Managing Cable Ageing in Nuclear Power Plants*, No. NP-T-T3.6, International Atomic Energy Agency, 2012. http://www-pub.iaea.org/MTCD/Publications/PDF/Pub1554_web.pdf.